EFFECT OF ADDING REARE EARTH ELEMENTS TO Mg-Ca BASE ALLOY ON CORROSION AND MECHANICAL BEHAVIOUR

Taher Ali Issa YOUSEF

2021
PhD THESIS
METALLURGICAL AND MATERIALS ENGINEERING

Thesis Advisor
Prof. Dr. Hayrettin AHLATCI

EFFECT OF ADDING REARE EARTH ELEMENTS TO Mg-Ca BASE ALLOY ON CORROSION AND MECHANICAL BEHAVIOUR

Taher Ali Issa YOUSEF

T.C
Karabuk University
Institute of Graduate Programs
Department of Metallurgical and Materials Engineering
Prepared as
PhD Thesis

Thesis Advisor
Prof. Dr. Hayrettin AHLATCI

KARABUK
June 2021

I certify that in my opinion the thesis submitted by Taher Ali Issa YOUSEF titled "EFFECT OF ADDING REARE EARTH ELEMENTS TO Mg-Ca BASE ALLOY ON CORROSION AND MECHANICAL BEHAVIOUR." is fully adequate in scope and in quality as a thesis for the degree of PhD.

Prof. Dr. Hayrettin AHLATCI   ....
Thesis Advisor, Department of Metallurgical and Materials Engineering

This thesis is accepted by the examining committee with a unanimous vote in the Department of Metallurgical and Materials Engineering as a PhD thesis. June.17.2021

Examining Committee Members (Institutions)   Signature

Chairman   : Prof. Dr. Mustafa ACARER (SU)   ....

Member   : Prof. Dr. Hayrettin AHLATCI (KBU)   ....

Member   : Prof. Dr. Ali GÜNGÖR (KBU)   ....

Member   : Assist. Prof. Dr. Cevat RAHEBİ (ASU)   ....

Member   : Assist. Prof. Dr. İsmail Hakkı KARA (KBU)   ....

The degree of PhD by the thesis submitted is approved by the Administrative Board of the Institute of Graduate Programs, Karabuk University.

Prof. Dr. Hasan SOLMAZ   ....
Director of the Institute of Graduate Programs

"I declare that all the information within this thesis has been gathered and presented in accordance with academic regulations and ethical principles and I have according to the requirements of these regulations and principles cited all those which do not originate in this work as well."

Taher Ali Issa Yousef

ABSTRACT

PhD. Thesis

EFFECT OF ADDING REARE EARTH ELEMENTS TO Mg-Ca BASE ALLOY ON CORROSION AND MECHANICAL BEHAVIOUR

Taher Ali Issa YOUSEF

Karabük University
Institute of Graduate Programs
Department of Metallurgical and Materials Engineering

Thesis Advisor:
Prof. Dr. Hayrettin AHLATCI
June 2021, 61 pages

Todays, light weight structure materials are the most important issue for the automotive and aerospace industry because of the rising environment problems such as CO_2 emission and efficient of energy consumption. (Mg) alloys can be the best alternative metallic materials which has both lower density and higher weight per density value than steel and aluminum. However, the main challenge of Mg material is the manufacturing process containing higher melting temperature than the its rival metals and extreme formability behavior due to the hexagonal structure. In this study, AZ31 and modified AZ31-x% (wt.) Ca, AZ31-x% (wt.) Ca-Ce alloys are produced. Homogenization was carried out at 400 °C for 24 hours after casting. Afterwards, slabs were removed from the homogenized logs to be 12x36x100mm. The slabs with an initial wall thickness of 12 mm were rolled at three different 1.5 m/min, 4.7 m/min and 10 m/min rolling speeds at 400 °C for each deformation rate with 15% deformation rate per pass. Optical microscope, SEM and XRD examinations of homogenized

materials were performed to determine the relationship between rolling capacity and microstructure. The microstructure of sheet materials that pass the rolling process and have a wall thickness of 2 mm was examined by optical microscope, SEM and the strength of the macro texture was measured using XRD. Besides, macro-hardness from mechanical tests test (HB) and tensile test at room temperature. In addition, potentio-dynamic and immersion corrosion tests were carried out in the 3.5% NaCl medium of the sheet material. In addition, abrasion tests were carried out at room temperature in a forward and backward direction in a dry environment. It has been observed that deformation amount per pass and different rolling speeds cause differences in grain size, twinning fraction and dispersion and size of sediments. The effects of the addition of alloying elements and microstructure properties on mechanical properties, corrosion resistance and wear behavior are examined.

ÖZET

Doktora Tezi

Mg-Ca BAZ ALAŞIMINA NADİR TOPRAK ELEMENTLERİ İLAVESİNİN KOROZYON VE MEKANİK DAVRANIŞ ÜZERİNE ETKİSİ

Taher Ali Issa YOUSEF

Karabük Üniversitesi
Lisansüstü Eğitim Enstitüsü
Metalurji ve Malzeme Mühendisliği Anabilim Dalı

Tez Danışmanı:
Prof. Dr. Hayrettin AHLATCI
June 2021, 61 sayfa

Günümüzde, CO_2 emisyonu ve enerji tüketiminin verimli olması gibi artan çevre sorunları nedeniyle hafif yapı malzemeleri otomotiv ve havacılık endüstrisi için en önemli konudur. Magnezyum (Mg) alaşımları, yoğunluk değeri başına çelik ve alüminyumdan daha düşük yoğunluk ve daha yüksek ağırlığa sahip en iyi alternatif metalik malzemeler olabilir. Bununla birlikte, Mg malzemesinin ana zorluğu, rakip metallerden daha yüksek erime sıcaklığı ve altıgen yapıdan dolayı aşırı şekillendirilebilirlik davranışı içeren üretim işlemidir. Bu çalışmada, AZ31 ve modifiye edilmiş AZ31-x% (ağ.) Ca, AZ31-x (ağ.) Ca-Ce alaşımları üretilmektedir. Homojenizasyon dökümden sonra 24 saat boyunca 400 ° C'de gerçekleştirildi. Daha sonra, plakalar homojenleştirilmiş kütüklerden 12x36x100mm olacak şekilde çıkarıldı. Başlangıç et kalınlığı 12 mm olan levhalar, geçiş başına % 15 deformasyon oranı ile her bir deformasyon oranı için 400 °C'de üç farklı 1.5 m/dak, 4.7 m/dak ve 10 m/dak haddeleme hızında haddelenmiştir. Homojenize malzemelerin optik

mikroskop, SEM ve XRD incelemeleri haddeleme kapasitesi ve mikroyapı arasındaki ilişkiyi belirlemek için yapılmıştır. Haddeleme işleminden geçen ve et kalınlığı 2 mm olan saç malzemelerinin mikro yapısı optik mikroskop, SEM ile incelenmiş ve makro doku mukavemeti XRD kullanılarak ölçülmüştür. Ayrıca, mekanik testler testinden (HB) makro sertlik ve oda sıcaklığında çekme deneyi. Ayrıca, sac malzemenin% 3.5 NaCl ortamında potansiyodinamik ve daldırma korozyon testleri yapıldı. Ayrıca, kuru bir ortamda aşınma testleri oda sıcaklığında ileri ve geri yönde gerçekleştirilmiştir. Geçiş başına deformasyon miktarının ve farklı yuvarlanma hızlarının tane büyüklüğü, ikizlenme fraksiyonu ve çökeltilerin dağılımı ve büyüklüğü bakımından farklılıklara neden olduğu gözlenmiştir. Alaşım elementleri ve mikroyapı özelliklerinin eklenmesinin mekanik özellikler, korozyon direnci ve aşınma davranışı üzerindeki etkileri incelenmiştir.

Anahtar Kelimeler : AZ31 (+ Ce), Sıcak haddeleme, Korozyon, Aşınma.
Bilim Kodu   : 91501

ACKNOWLEDGMENT

I would like to reveal my major thanks of gratitude to my advisor Prof. Dr. Hayrettin AHLATCI who gave me the glorious moment for the extended support of my Ph.D. research and detailed analysis, for his perseverance, interest, and tremendous insight. I am absolutely grateful to him. Besides my advisor, I would like to thank the rest of my thesis committee: Prof. Dr. Ali Güngör, and Dr. Ismael Hakki KARA, for their encouragement, insightful comments, and hard questions.

Finally, I would like to give special and grateful thanks to my wife for her support and patience during this long journey, without her encouragement I would not have been able to continue.

CONTENTS

LIST OF FIGURES

LIST OF TABLES

SYMBOLS AND ABBREVITIONS INDEX

SYMBOLS

Al : Aluminum

Ca : Calcium

Li : Lithium

Mg : Magnesium

Mn : Manganese

Fe : Ferrous

Zn : Zinc

Ni : Nickel

Ce : cerium

Ta : Tantalum

Alumina : Al_2O_3

A12 : $Al_{12}Mg_{17}$

C14 : Mg_2Ca

C15 : Al_2Ca

ABBREVITIONS

EDS : Energy Dispersive X-ray Spectroscopy

HCP : Hexagonal Close-Packed

RE : Rare earth elements

SEM : Scanning Electron Microscope

SCC : Stress Corrosion Cracking

UTS : Ultimate Tensile Strength

XRD : X-Ray Diffraction

XRF : X-Ray Fluorescence

Y.S : Yield Strength

MPa : Megapascal

log : logarithmic

PART 1

INTRODUCTION

Magnesium alloy was used as the building material of aircraft especially in World War I and II. The Mg alloys, which continue their attractiveness in the world war, have been replaced by aluminum alloys in the following periods due to the reasons such as ore amount and production cost. However, it has recently brought up the use of Mg alloys again due to increased CO_2 emissions and reduced energy efficiency, lightness and special strength. Mg alloys, used primarily in the automotive industry and aviation applications, are indispensable in our daily lives, even in the cases of devices such as mobile phones and laptops. The product range of Sheet Mg alloys covers a wide range. However, it is of great importance to develop Mg alloys that are weak in room temperature due to HCP structure and to reduce production costs. In recent years, alloying has created a wide field of work to produce Mg alloys that have good shaping ability at low temperatures and have strong mechanical properties. The weakening effect of elements such as Cerium, Gadolinium, Yttrium and Neodymium, which are known as rare earth elements, was determined in pure Mg and it was provided to take shape more easily. Ce, Nd and Gd, were used to improve the AZ31 Mg alloy rolling capability, which is the most widely used among AZ series, and positive results were obtained.

The aim of this study is primarily to produce AZ31 Mg alloys containing Ca and Ce by low pressure casting method. Afterwards, the rolling of the alloys produced using different rolling parameters is the production of materials with weak texture, that is, easier to form, higher strength and better corrosion resistance and wear behavior compared to the AZ31 Mg alloy.

This thesis content is the introduction part in the first chapter and a summary of the study is given here. In the second chapter the literature reviews is examined and previous studies are evaluated.

In the third, chapter, experimental part was presented. In the fourth section, the results of the experiments are given in the form of tables, graphics and the results and literature comparison. In the last part, general results obtained from the study are discussed and conclusion given.

PART 2

MAGNESIUM ALLOYS

2.1. GENERAL FEATURES

The discovery of magnesium (Mg) dates back to 1755. Scottish scientist Joseph Black first discovered the magnesia mineral containing magnesium. However, British scientist Humphrey Davy first provided the isolation of magnesium in 1808 and was honored as the inventor of magnesium. For the first time, Germany became the state that produces Mg products. During the First World War, other developed countries started the production of magnesium. II. The production of Mg alloys with increasing production until World War II. Its use decreased after World War II. The most important success of Mg alloys, which have potential for use in many fields, has been achieved with the WV brand Ferdinand Porche model. Extrusion product Mg alloys found the opportunity to be used in daily life products such as scaffolding, wheelbarrows, chainsaws and oven racks. Rolled product Mg alloys were produced in 1950s for aircraft and rockets. Today, the use of Mg is popular in cars, home appliances and sports applications. Magnesium atom in its outer shell has only 2 electrons, so it can lost them easily and become positively charged [1]. The most important factor in this is its lower density (1.74 g / cm3) compared to aluminum. However, its production cost is high, its shaping ability is low and its corrosion resistance is problematic [2] [3].
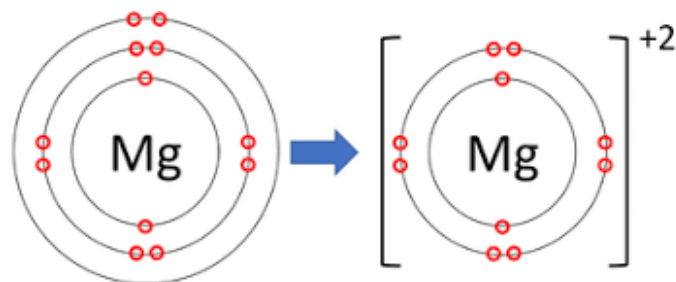
Figure 2.1. Magnisum elecrton configration.

2.2. MAGNESIUM ALLOYS AND STANDARDS

ASTM system is used for classification of Mg alloys. Letters and their composition represent the main elements of their alloys. For example, AZ31 contains 3% aluminum and 1% zinc.

- ASTM system is used for classification of Mg alloys as Following
- XXNNE T:

1. XX, Indicates the two principal alloying elements
2. NN, Indicates the amount of the two principal alloying elements
3. E, Distinguishes between different alloys with the same percentages of the two principal alloying elements
4. T, Indicates Treatment condition (temper)

Table 2.1. ASTM codes used for elements of magnesium alloys [1].

Abbreviation	Alloy element	Abbreviation	Alloy element
A	Aluminum	N	Nickel
B	Bismuth	P	lead
C	Copper	Q	Silver
D	Cadmium	R	Chromium
E	Rare earth	S	Silicon
F	Iron	T	tin
H	Thorium	W	Yttrium
K	Zirconium	Y	Antimony
L	Lithium	Z	Zinc
M	Manganese		

2.3. MG ALLOYS SUITABLE FOR PLASTIC SHAPING

The shaping ability of Mg alloys is very weak because of HCP structure and twins. Therefore, few Mg alloys suitable for shaping [1].

Table 2.2. Mg alloys suitable for shaping [1].

Abbreviation	Al	Ca	Zn	Mn	Cu	Zr	Y	Nd	Th
AZ21X1	1, 6-2,5	0,1-0,25	0,8-1,6	0,15 maks	0,05	-	-	-	-
AZ31	3	-	1	0,3	-	-	-	-	-
AZ31B	2,5-3,5	0,04 maks.	0,7-1,3	0,2-1,0	0,05	-	-	-	-
AZ61A	5,8-7,2	-	0,4-1,5	0,15-0,5	0,05	-	-	-	-
AZ80	8,5	-	0,5	0,12	-	-	-	-	-
AZCOML	2,0-3,6	0,04 maks.	0,3-1,5	0,15 min.	0,10	-	-	-	-
AZM	6,0	-	1,0	0,3	-	-	-	-	-
ZC71	-	-	6,5	0,7	1,2	-	-	-	-
ZK40	-	-	3,5-4,5	-	-	0,45 min	-	-	-
ZK60A	-	-	4,8-6,2	-	-	0,45 min	-	-	-
ZM21	-	-	2,0	1,0	-	-	-	-	-
ZW3	-	-	3,0	-	-	0,6	-	-	-
HM21	-	-	-	0,8	-	-	-	-	2,0
HM31	-	-	-	-	-	0,7	-	-	2,0
WE43	-	-	-	-	-	0,5	4,0	4,0	-
WE54	-	-	-	-	-	0,5	5,25	3,5	-

2.4. THE EFFECT OF ALLOY ELEMENTS

Solid melt hardening and precipitate hardening are effective in improving the mechanical properties, casting ability, corrosion resistance and microstructure of magnesium. The amount of alloying elements is controlled in a molten state, taking

into account the solubility of each element. The effects of alloying elements are listed below [4].
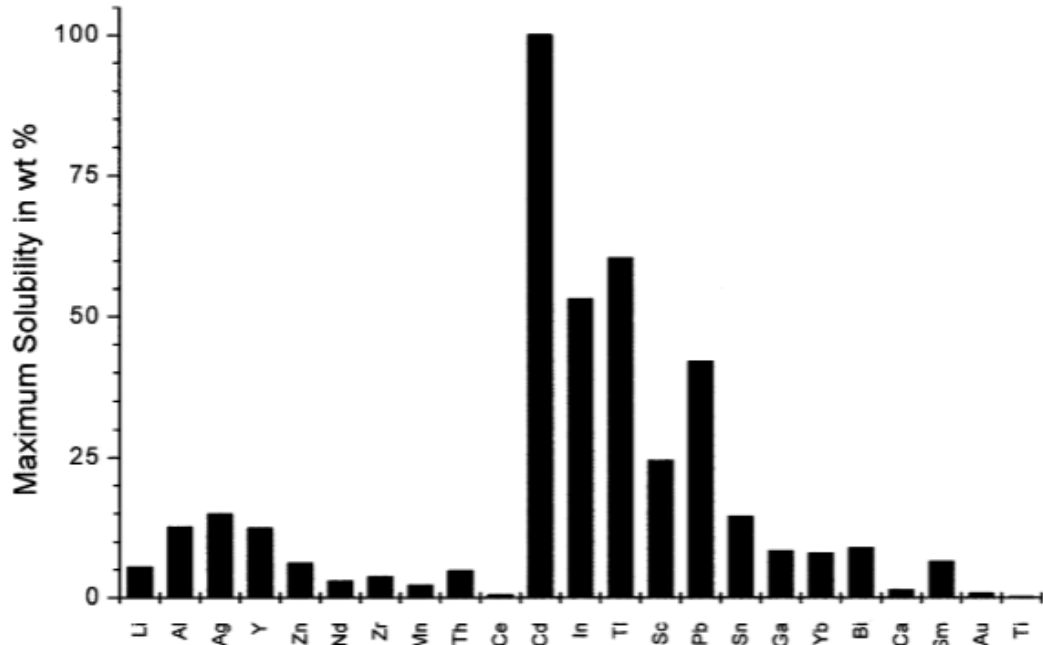
Figure 2.2. Maximum solubility(%wt) amounts of the elements in Mg at room temperature [5].

2.4.1. Aluminum

It is the most widely used alloy element. It improves casting ability and mechanical properties. Its solubility in Mg is 2.6% w / w at room temperature and 12.1% w / w at 436 ° C. This reduced resolution from the eutectic temperature gives the alloy heat treatment and aging ability. $Mg_{17}Al_{12}$ precipitate and solid melt Al are effective in improving mechanical properties. Its main disadvantage is that it increases microporosity. The Al content of many Mg-Al alloys is in the range of 2-9% and an optimum 6% is recommended [4]. Aluminum improves corrosion behavior because it modifies the composition of the of the hydroxide film on the surface [6].

2.4.2. Beryllium

It is used with Mg alloys in traces (around 10 ppm) which prevents oxidation. Also it,s known as iron remover. However, it lead to grain growth in Mg-Al alloys [7].

2.4.3. Calcium

It is added to improve mechanical properties and used effectively in improving creep resistance and grain thinning [8].

2.4.4. Copper

It negatively affects the corrosion resistance of Mg-Al-Zn alloys. However, it affects the ductility of Mg-Zn alloys well and improves aging ability. It also contributes to high temperature resistance [9].

2.4.5 Nickel and Iron

It is important that there is a trace amount due to damage to the corrosion resistance [4].

2.4.6. Lithium

Its main advantage is that it improves its shaping ability. However, on the other hand, it decreases the mechanical properties and corrosion resistance [10].

2.4.7. Manganese

It reacts with iron and reduces free iron atoms in the structure and thus contributes significantly to corrosion resistance [11].

2.4.8. Silicon

It improves the fluidity of the molten metal. However, the trace amount of iron it contains affects the corrosion resistance [4]. However, AZ61 Mg improves both the mechanical and bio-corrosion properties of the alloy [12].

2.4.9. Silver

It increases high temperature resistance and creep resistance together with rare earth elements. It also improves mechanical properties due to its aging ability [13].

2.4.10. Zinc

It is the second best alloying element. Together with aluminum, it improves room temperature resistance. In addition, the corrosive properties of iron and nickel decrease with the addition of zinc [4]. In addition, it improves the aging ability [14].

2.4.11. Zirconium

It has a thinning effect. It improves strength without damaging the ductility [15]. However, it is not used in alloys containing Al or Mn. Because Al and Mn in solid melt form a precipitate and remove it from the structure [16].

2.4.12. Cerium

Cerium, on the contrary, is known to improve the strength and elevated temperature properties of magnesium alloys. Promising creep performance has been observed in Mg–Mn–Ce alloys in the past and these have been mainly used in the nuclear reactor Industry, it can be inferred that magnesium alloys containing both Mn and Ce constitute a good base for the development of casting and wrought alloys [17].

2.5. BINARY DIAGRAMS

2.5.1. Aluminum

The Mg-Al phase diagram includes the liquid phase, the solid phase with the HCP structure, and the R phase. Al dissolves at most 18.9% (be atomic) at 450 °C [17].
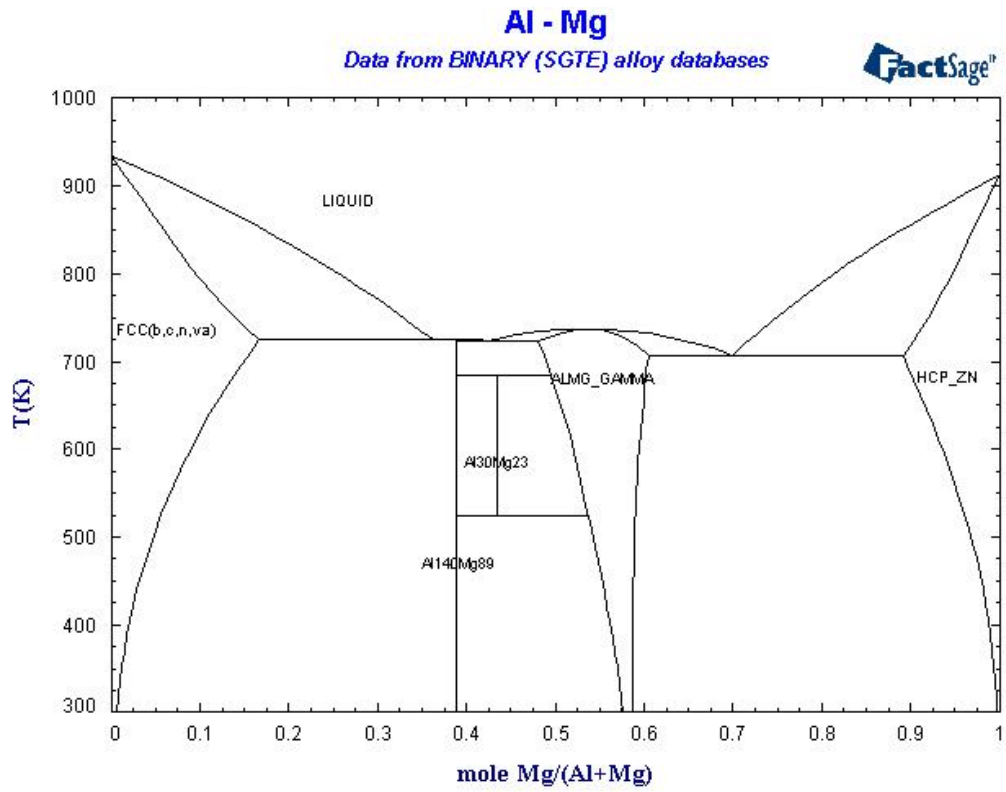
Figure 2.3. Mg-Al phase diagram [18].

2.5.2. Manganes

It dissolves at a maximum of 2% (atomic) at 653 °C. There is no medium composition in the Mg-Mn binary phase diagram [17].

Mg - Mn
Data from FTlite - FACT light alloy databases
FactSage
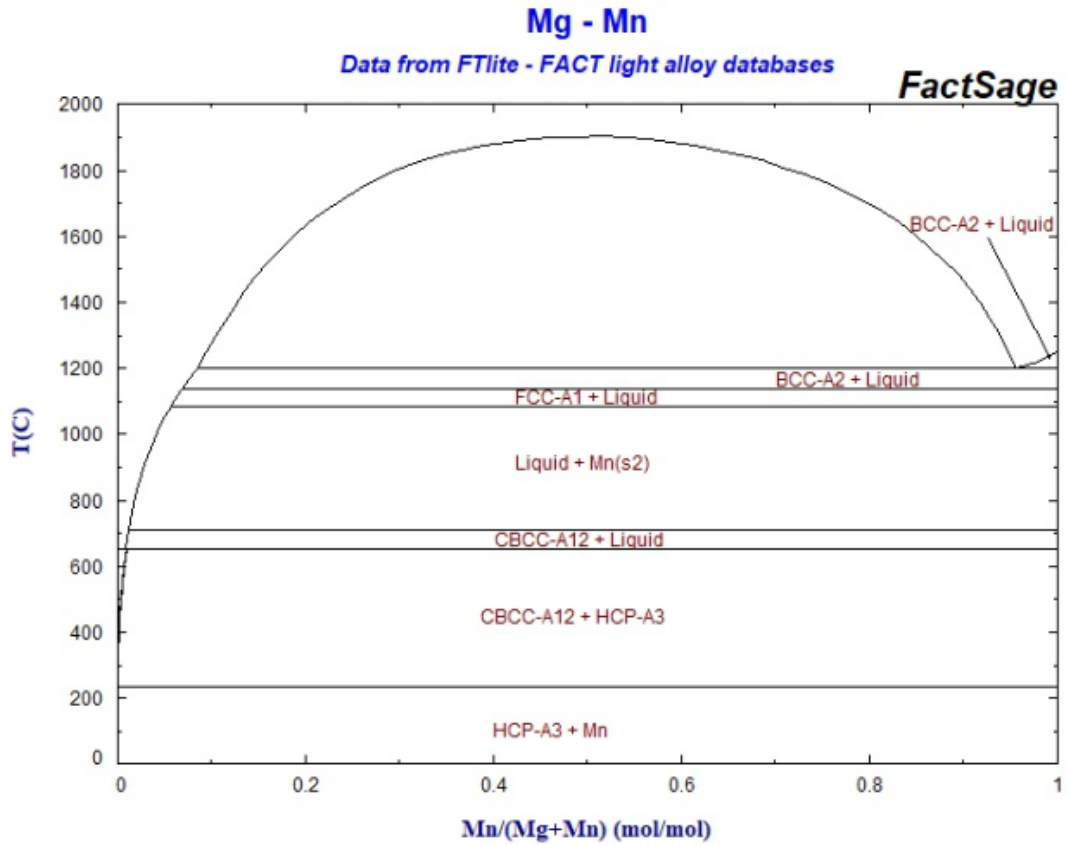
Figure 2.4. Mg-Mn phase diagram [18].

2.5.3. Zinc

MgZn2 phase dissolves at 595 °C. This phase is eutectic in the content of 97% (at.ol.) Zn at 368 °C. There are no solid melt sites in this system [17].
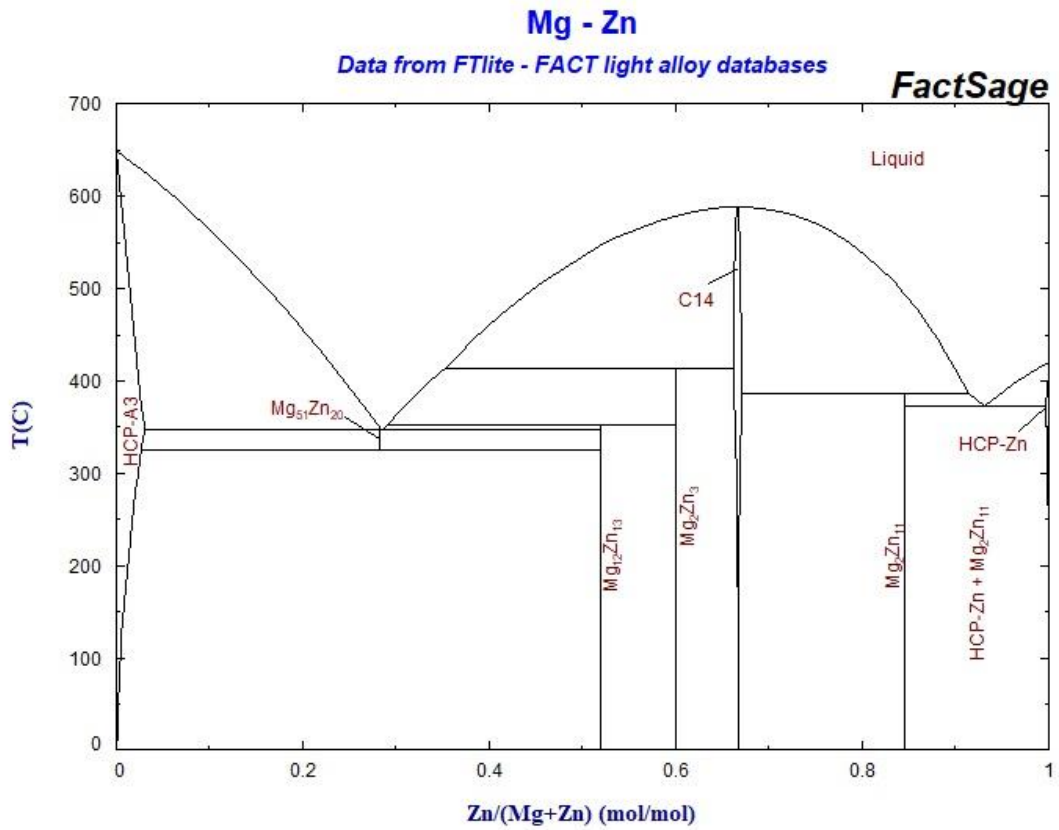
Figure 2.5. Mg-Zn phase diagram [18].

2.5.4. Calsium

It has very low solubility in Mg and has a very high eutectic temperature (722 °C). It does not improve aging ability due to its low dissolution [19].
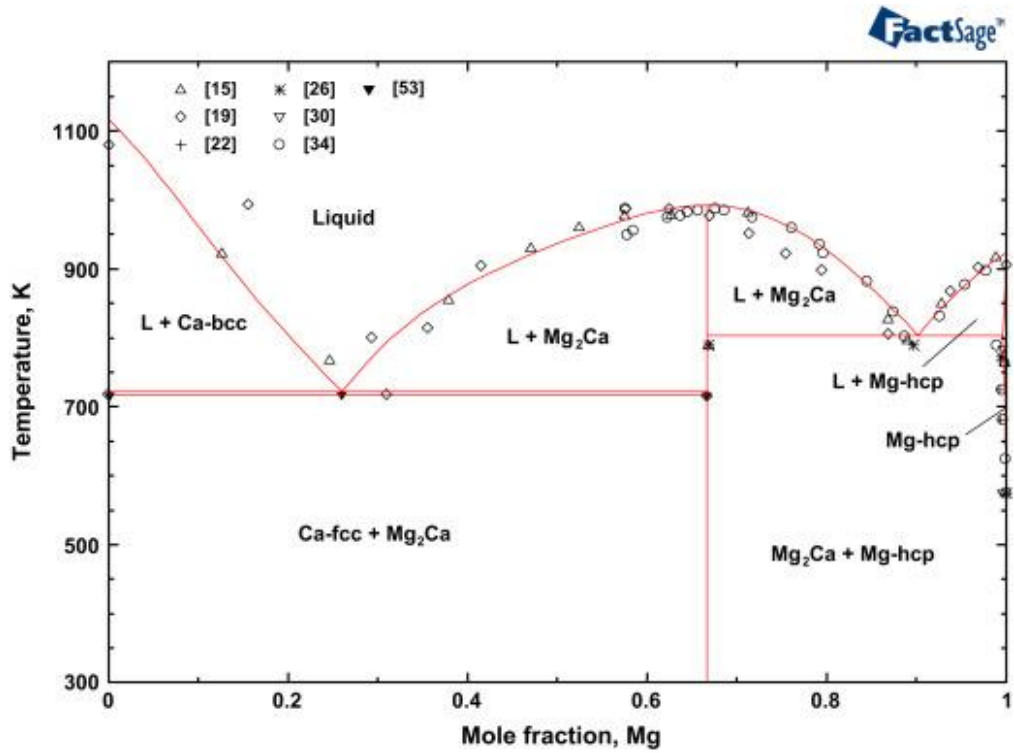
Figure 2.6. Mg-Ca phase diagram [20].

2.5.5. Cerium

It has a good solubility in mg and has the lowest eutectic temperature (505 °C). Improves aging ability. The secondary phase of is very hard and provides better creep strength.
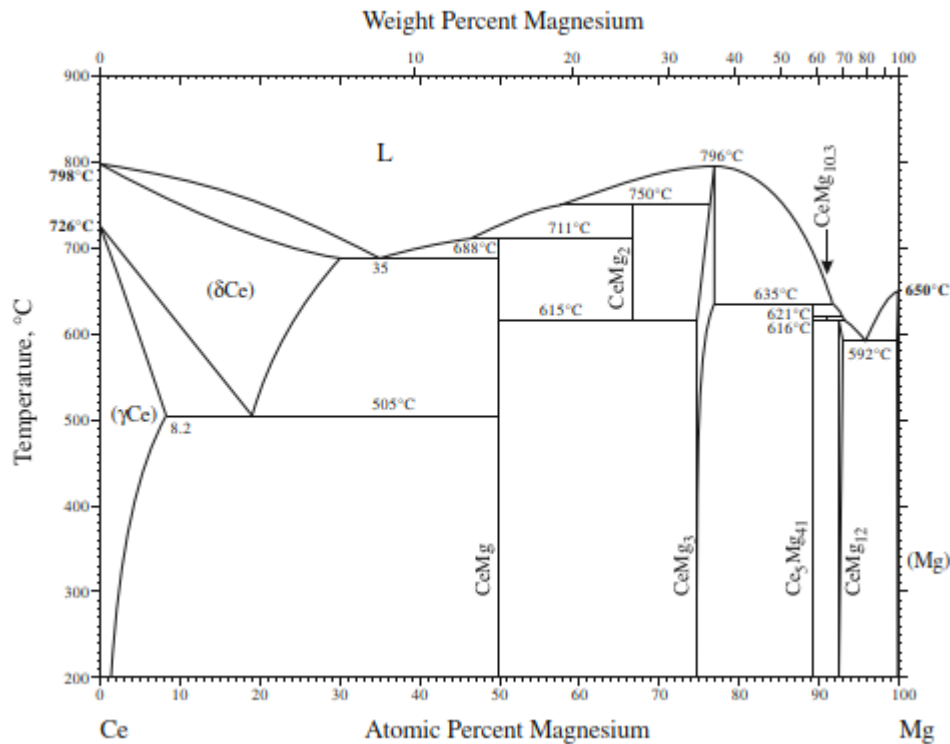
Figure 2.7. Ce - Mg phase diagram [18].

2.6. MAGNESIUM ALLOYS CASTING METHODS

2.6.1. Casting into High Pressure Coil Mold

Thanks to this casting method, which is known to provide great convenience in the production of light metal parts, Mg parts with a thick and thin wall thickness are easily produced. There are two types of mold casting in hot and cold mold. Oxidation is difficult to form since the molten metal is prevented from coming into contact with the air in the hot die casting mold method. Mg and steel are particularly compatible with the 400 series. The steel molds used here provide the production of high strength material. Cold mold permanent mold provides comfort in the production of Mg alloys

that are excessive in volume and clear. However, alloys containing very little gaps are produced in these two casting processes. In order to prevent this, vacuum casting mold method has been developed [3].
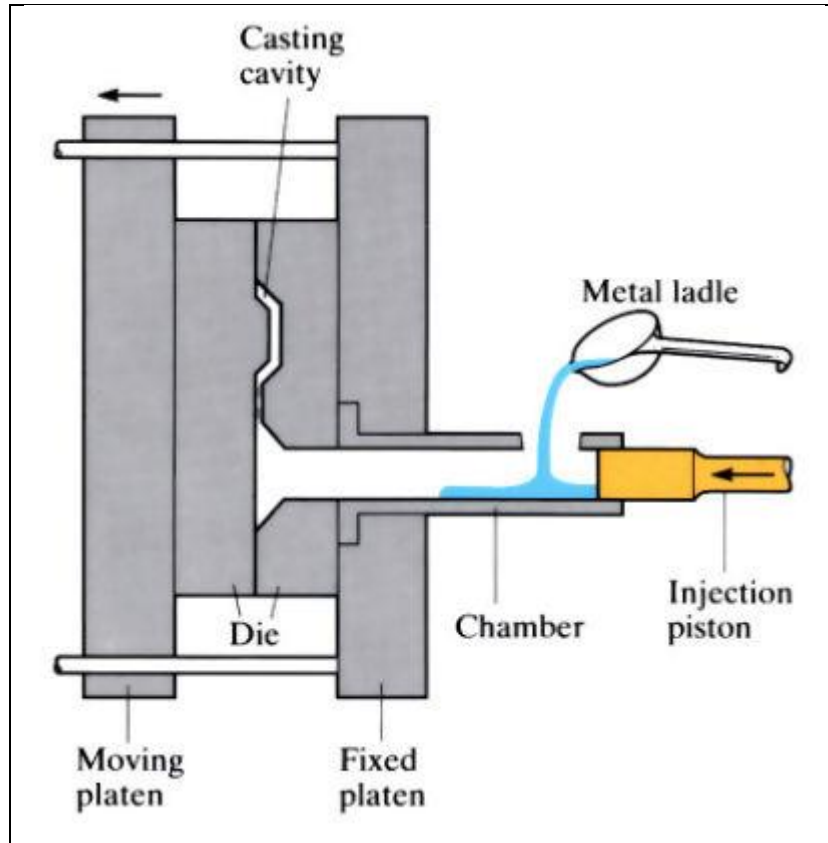
Figure 2.8. Casting into high pressure die mold [18].

2.6.2. Casting by Gravity

Although high pressure permanent mold casting is popular, sand or permanent mold casting methods are also used in the production of some Mg parts. With the sand casting method, parts weighing up to 1.5 tons can be produced. Here, the cost of production is low, but since Mg has low density, its nutritious and runner design requires significant expertise. In permanent mold casting, it enables more solid parts to be produced because it provides fast solidification [3].

2.6.3. Casting In Low Pressure Coil Mold

In the low pressure permanent mold casting method, the molten metal is designed to be at the bottom and the mold at the top. The molten metal is injected into the mold by pressure. The pressure applied is gradually increased after the mold starts to fill and after the mold is filled, the pressure is cut off. Here, the design for the feeder system requires expertise. Because, after the mold is filled, the increased melt metal should return to the pot again without solidification. Thanks to this casting method, internal cavities are almost completely prevented. Low pressure casting is preferred for the production of parts requiring hollow space. But the low pressure casting method is designed for aluminum alloys. The production of Mg alloy parts has been carried out, and a more robust product has been obtained compared to the sand casting method [3].
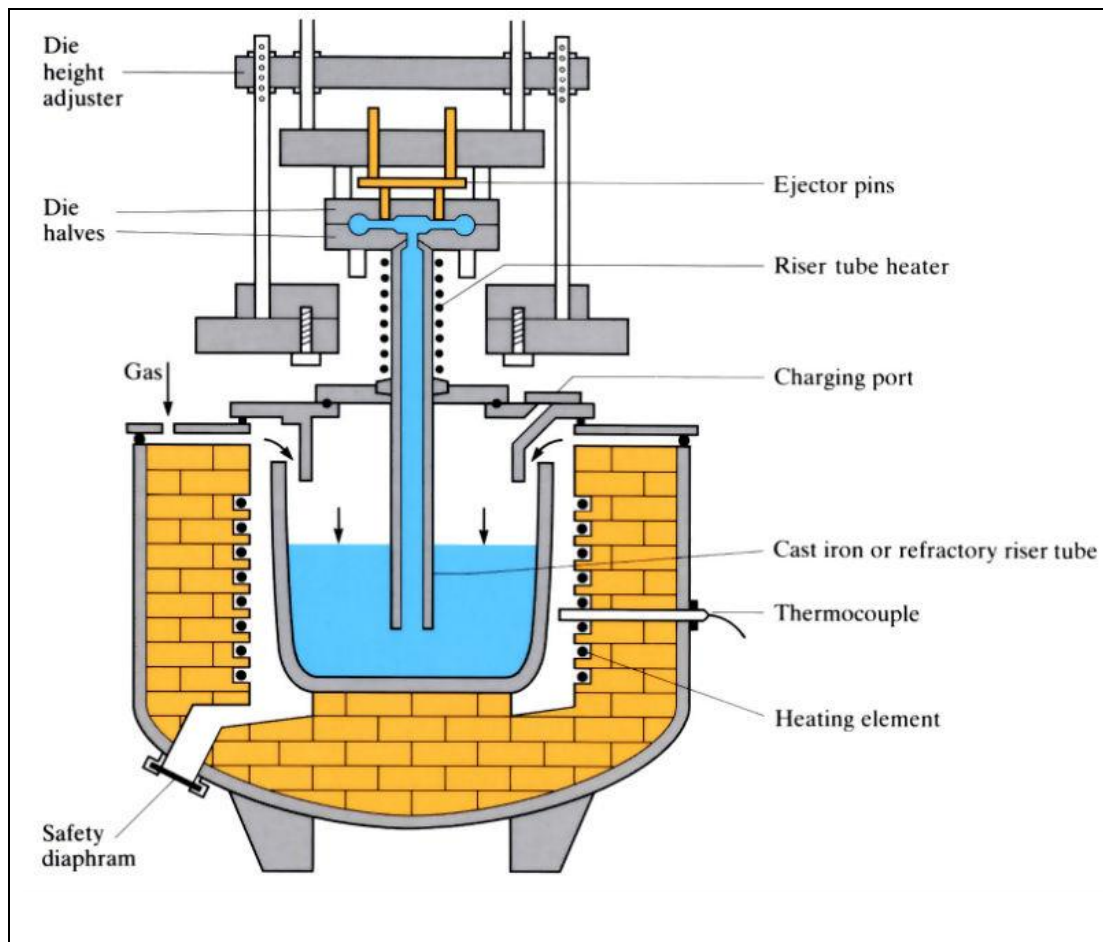
Figure 2.9. Low pressure mold casting into mold [18].

2.7. USAGE AREAS OF MAGNESIUM ALLOYS

The first use of Mg alloy is seen in military applications. Nowadays, it has spread to areas where less energy consumption and lower gas emission are needed, especially in the automotive sector. The history of Mg alloys in the automotive industry dates back to the 1920s. The first application is the engine pistons of the Indy 500 race car in America. About 4 million pieces of Mg pistons were produced in Germany in 1937. Another Mg track sump was produced in 1931 by the general engine. Towards 1970, gearbox and air cooled engine applications took place in the automotive industry. Increased engine power and overheating have led to the use of water-cooled engines instead of air-cooled engines, so the use of Mg parts has begun to decrease. Despite this, applications such as Mg seat frame, passenger door and steering frame continue to be produced by brands such as Mercedes and BMW since 1990's. In addition, it is an ideal alloy for all portable electronic devices [3].
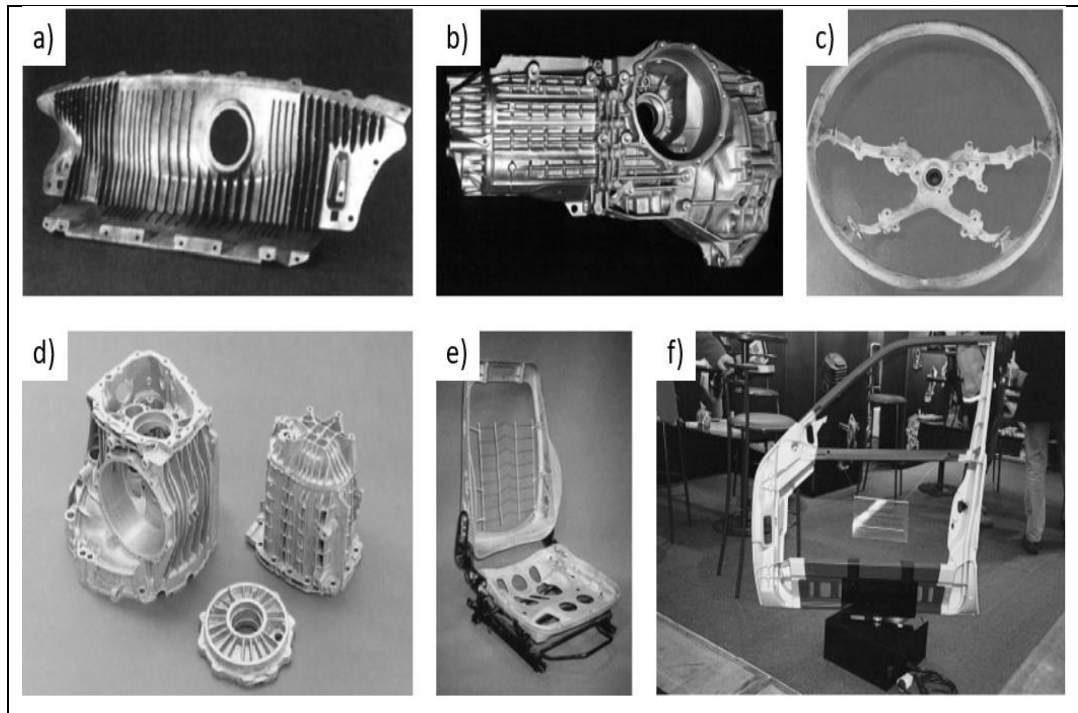
Figure 2.10. Magnesium auto parts, a) Fuel tank protector, b) Gearbox c) Steering frame d) Gearbox e) Seat frame and f) Passenger door frame [1].
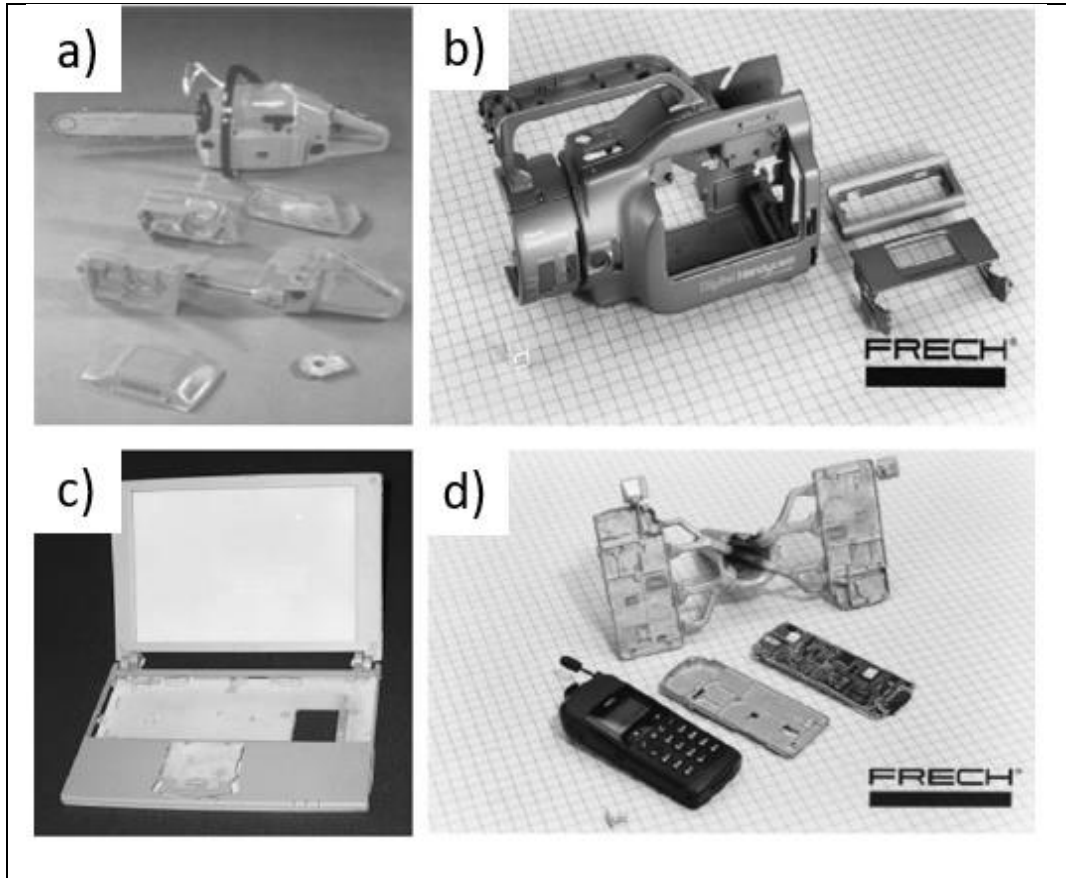
Figure 2.11. Magnesium electronic parts a) Saw, b) Camera, c) Laptop and d) Mobile phone [1].

2.8. Mg SHEET PRODUCTION WITH TRADITIONAL MATERIAL METHOD

In the conventional route for producing Mg sheet, the process is generally as follows: i) direct cooling (DC) casting process up to cast molds (eg 0.3m x 1m x 2m); ii) homogenizing the plates for several hours (eg at 450 °C); iii) hot rolling (480 °C ~ 300 °C) in several passes up to 5-6 mm in a reverse hot mill; iv) the final finish is rolled in several passes of a 5-20% reduction by annealing the sheet (typically at 340 °C) before each final pass. The last part of hot rolling is time consuming, limits productivity and has a high operating cost [21].

2.8.1. Rolling Parameters

The amount of deformation per temperature and pass is very important. In addition, strain rate and rolling rate are other parameters affecting the result microstructure.
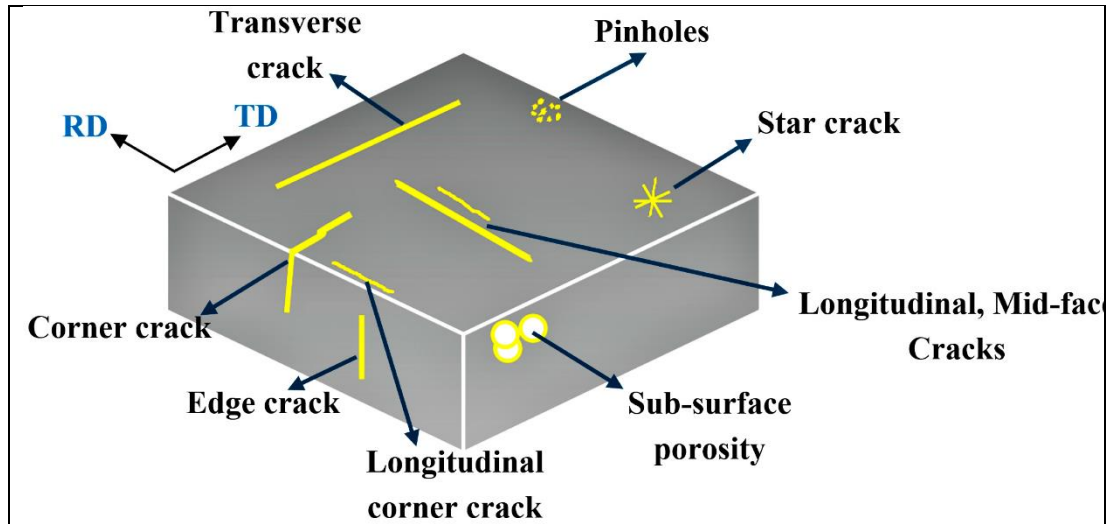
Figure 2.12. Typical surface defects in rolled products (RD: rolling direction, TD: transverse direction) [22].

Gou F. et al. They have rolled the AZ31 Mg alloy between 3 m / min-12.1 m / min rolling speeds in three different rolling speeds at 20%, 40% and 70% deformation rates in one pass. It has been reported that small deformation causes twinning but recrystallization is dominant with increasing deformation. It has been reported that recrystallization increases ductility but increased twinning fraction decreases ductility but contributes to yield strength [23]. In addition, the same author said in another study that recrystallization at high rolling speeds expanded and distributed homogeneously, but recrystallization at low rolling speeds was limited in slip bands. In addition, it was reported by the same author that dynamic recrystallization prevents edge cracks during rolling [24]. Ding Y. et al. They applied AZ31B Mg alloy to rolling mill speeds of 18m / min -102m / min. Twinning and continuous dynamic recrystallization were observed during deformation. Along with the increasing rolling speed of the material rolled in a total of 4 passes, twinning density decreased, but grain growth occurred due to preventing the sudden change in temperature change. The grain size of the material rolled in a total of 2 passes increased too much, but recrystallization decreased. While

the temperature decrease on the surface of the material was lower at the rolling speed of 102m / min, the temperature increase in the interior of the material was said to be higher, so that the total amount of heat lost by the material during the rolling was decreased. In addition, it is reported that the materials passing through a large number of passes are exposed to this effect more in the last two or three passes. Here, edge formation and twinning decreased while grain size increased [23].

Another important parameter, the deformation rate, Liu Di. et al. It has been worked on AZ31 Mg alloy. The material of 26mm thickness was rolled at a rate of 3.5m / min at 350 ° C at 15%, 20%, 25% and 30% per pass and 4mm sheet metal was obtained. Thinning was obtained in the grains due to the increasing deformation rate. In addition, it has been reported by the authors that fine grains and strong textures increase strength, but weak textures and fine grains are required for more ductile material [25]. Kim W.J. et al. They obtained 0.6mm thin sheet by deforming 2mm thick sheet 70% in one pass. As a result, they achieved AZ31 Mg alloys superior in strength and ductility [26]. On the other hand, Huang X. et al. They reduced the thickness of the 2mm wall thickness of the AM60 and AZ61 alloys by a total of three passes by 26% per pass, by 0.8mm. Here, AZ61 was rolled at 505 °C and AM60 at 480 °C in the first two passes and 545 °C at the last pass. The materials were then annealed at 350 °C for 1 hour. It has been reported that the AZ61 alloy has a stronger texture than the AM60 alloy, and this is said to be caused by the solid melt soluble Zn element [27]. Wei et al. The effect of strain rate on the superplastic and grain boundary shear properties of AZ91 Mg alloy, which has undergone the rolling process between the strain ratio between $\{10\}^{\{-3\}}$ and $\{1s\}^{\{-1\}}$, was investigated. As a result of the study, the high strain rate of superlasticity developed and the strain rate of $\{10\}^{\{-3\}} s^{\{-1\}}$ at 350 °C provided a 455% elongation. It is stated here that grain boundary shift is the most important mechanism for plastic deformation [28].

2.8.2. The Effect of Alloy Elements on Rolling Capability

Rare earths (NTE) and combinations have been the most widely used alloy strategy for Mg, as it is most effective in reducing texture densities and improving ductility. As a result of reduction of twinning volume fraction, anisotropy and asymmetry decrease will be observed. In addition, increasing the ductility of Mg-NTE alloys at room temperature contributes to the activation of non-basal sliding systems. Thus, the tendency to deformation twinning is reduced. On the other hand, NTE texture modification greatly affects recrystallization. In addition, particle-induced nucleation (PSN) is promoted through NTE. Prevention of recrystallization during the thermo-mechanical process and the formation of a large number of slip bands are created by the NTE, where large spreads occur. However, there are also Mg-NTE alloys that do not contain a slip band but trigger the PSN mechanism [29].

W. P. Li et al. They investigated the rolling ability and effect of the gadolinium element on the microstructure of the AZ31 alloy. They added 1% Gd, 2% Gd and 3% 3Gd to the AZ31 alloy as mass fraction. As a result of microstructure analysis, α-Mg matrix and irregular β phase ($Mg_{17}Al_{12}$) precipitation were observed along the grain boundaries in AZ31 alloy after casting. In addition, spot-like sediments were encountered. As a result of the EDS analysis, it was revealed that the spot-like precipitate was rich by Al-Mn. With the addition of Gd, it was observed that the volumetric fraction of the β phase decreased and changed in the form of small particles. In addition, polygonal-like Al-Gd rich sediments were encountered. As a result of the XRD analysis, it was understood that this precipitate was Al_2Gd. With the addition of increasing Gd, the amount of β phase decreased but it was observed that the amount of Al_2Gd precipitate increased. As a result of XRD analysis, it was revealed that AZ31-% 3Gd composition does not contain the β phase. As a result of the average grain size analysis, it has been understood that the average grain sizes of AZ31, AZ31- 1% Gd, AZ31-% 2Gd and AZ31-% 3Gd casting alloys are 87μm, 51μm, 43μm and 46μm, respectively. It has been observed that after the homogenization process, many β phases dissolve in the matrix and the amount of çözün phase dissolved with increasing homogenization time. It was found that the composition containing 2% Gd dissolved more fazla phases than the AZ31 alloy. It is explained that with the addition of increasing Gd, the β phase changes in the form of small particles and these small particles dissolve more easily in the matrix. However, it has been observed that Al_2Gd

precipitate dissolves very hard in the matrix and after homogenization, AZ31-2% Gd alloy still contains finer grains than AZ31 alloy. In addition, it was reported that the shape and distribution of the precipitate phases were more uniform and homogeneous in the composition of AZ31-2% Gd. When the microstructure of rolled AZ31% XGd alloys is examined, it is said that paired small-grained structures are formed in all samples. It is written that this is due to the dynamic recrystallization during the rolling mill. The rolled AZ31, AZ31% 1Gd, AZ31-% 2Gd and AZ31 +% 3Gd alloys were found to have average grain sizes of 13.2μm, 9.5μm, 6.3μm and 8.1μm, respectively. It is reported that the original first grain size has a significant effect on the size of the dynamic recrystallized grains. It is also reported that the presence of Al_2Gd precipitate is present in the grain boundaries of AZ31-Gd alloys. Rolling ability in the study was evaluated as maximum thickness reduction and maximum thickness reduction per pass. It was reported that there was an increase with the addition of Gd for both results. The alloy with the best rolling ability is said to be AZ31 + 2% Gd. It is stated that one of the main reasons for this is the shape and distribution of the sediments. It is stated that the more regular shape and more homogeneously dispersed sediments have less cracking. It has been reported that the reduction of the β phase is important in terms of improving the rolling ability, and cracks are formed as a result of the β phases having irregular shape during the rolling exposure to different deformation strains. They attributed the first to excessive Al_2Gd deposits due to the fact that the AZ31 +% 3Gd alloy is weaker than the AZ31 +% 2Gd alloy in terms of rolling ability. They stated that the excessive Al_2Gd precipitates would negatively affect the ability to roll, as they would produce too much stress concentration, thereby causing microcracks. The other reason is that they are attributed to grain reduction. The fact that there are more units per unit volume shortens the dislocation sliding distances, which is a positive contribution to the ability to roll. Indirectly, Al_2Gd sediments have been said to play a role in the contribution of the small grains to the rolling ability, as DRXs increase [30].

In another study, W. Li et al. They studied AZ31-Ce-Gd alloys and examined the effect on Ce and Gd microstructure and roll ability. The alloys they examined are AZ31, AZ31 + 0.35Ce, AZ31 + 0.35Ce + 1.5% Gd and AZ31 + 0.35Ce + 0.35Gd. As a result of microstructure studies, it is said that the smallest grain size (40μm) alloy is 0.331% Ce + 1.5% Gd AZ31 alloy. It is mentioned that the casting product AZ31 consists of

α-Mg matrix and β-Mg$_{17}$Al$_{12}$ phases that precipitate at irregular grain boundaries. It is reported that the α-phase contains coarse dendrites. With the addition of Ce, the volumetric fraction of the β-phase is said to be reduced and dispersed into smaller particles. In addition, the rod-like phase was observed. With the addition of Gd to the alloy, the β-phase decreased more and the rod-like phase still remained. In addition, polygonal-like phases were observed. Cluster-like phases appeared with increasing Gd amount. XRD analysis revealed that the rod-like phase is Al$_4$Ce, the polygonal-like phase is Al$_2$Gd and the cluster-like phase is Mg$_3$Gd. It was observed that the β-phase dissolved in the matrix after homogenization. In addition, the precipitate phases in AZ31Ce-Gd alloys are said to be more uniform and homogeneous in shape and distribution than the AZ31 alloy. After homogenization, Al$_4$Ce, Al$_2$Gd and Mg$_3$Gd are reported to dissolve very little in the matrix and are stable even at high temperatures. It was also reported that after the homogenization process, the AZ31-Ce-Gd alloys still have smaller grains than the AZ31 alloy. It is mentioned that the grains shrink after rolling and they are smaller than 15 μm. The alloy with the smallest grains is said to be AZ31- 0.35Ce- 1.5% Gd. It has been written that the formation of coaxial grains in all rolled alloys is indicative of dynamic recrystallization. In addition, it is reported that the coaxial grains are more in AZ31-Ce-Gd alloys. In this study, the rolling ability of the alloys was evaluated on two factors: maximum thickness reduction and maximum thickness reduction in a pass. AZ31 alloy was applied with high strain rolling (53%) and cracks were observed. The same deformation amounts were applied to the alloys AZ31- 0.35Ce- 1.5% Gd but no cracks were observed. It was reported that the maximum thickness reduction and maximum thickness reduction per pass increased with increasing amount of Ce and Gd. It has been written that the alloy with the best rolling ability is AZ31- 0.35Ce- 1.5% Gd. Its ability to roll is based on the shape and distribution of the sediments. Alloys with more regular and more homogeneous distribution are said to have less risk of cracking during rolling [30].

2.9. TYPES OF CORROSION

Galvanic corrosion; it is the most common and damaging type of corrosion. Mg alloys act as anodes when combined with other engineering metals due to their negative corrosion potential as in Fig. (2.12). The most important factor in galvanic corrosion

is the potential difference between the anode and cathode. Besides, anodic and cathodic polarization resistance is another important factor. As it is known, Fe, Ni, Co, Cu, W, Ag and Au act more noble than Mg alloy in aqueous solution. The most and least harmful for Mg alloy used with aluminum, steel and sometimes copper are steel and aluminum respectively. Besides, Mg alloys can be galvanic corrosion even in itself. Electrochemical activities result in the formation of galvanic pairs, depending on the micro scale composition, microstructure and crystal orientations. Here, the phase or composition in which the anode or cathode behaves can change. However, the particles in the Mg alloy, which generally contain trace amounts of alloys as secondary phases, intermetallic and impregnated particles, act as micro anodes [31].
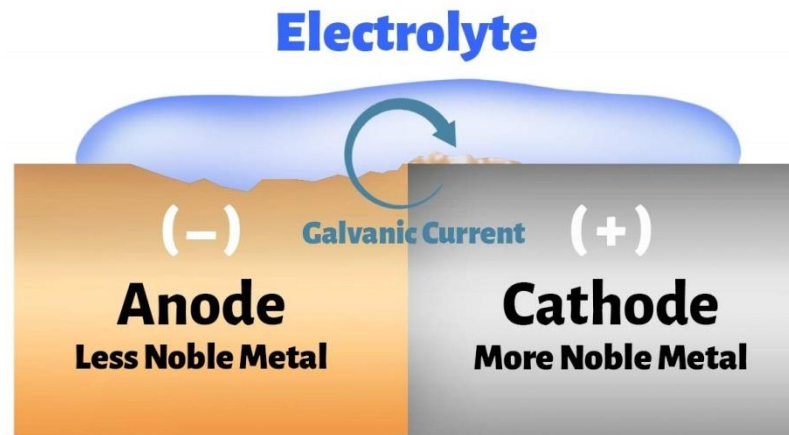
Figure 2.13. Typical surface defects in rolled products (RD: rolling direction, TD: transverse direction) [22].

Pit corrosion; The inhomogeneous crystal structure, for example, Mg alloy containing the secondary phase of $Mg_{17}Al_{12}$ causes the start of pit corrosion. Such secondary phases show higher standard voltages and go into electron exchange with the Mg matrix around it. Corrosion morphology in the form of holes emerges here [1].

Feng et al. They investigated the effect of secondary phases on the corrosion resistance of AZ series Mg alloys. In the study, it is reported that the secondary phases are formed within the grain and grain boundaries and act as micro-cathodes. This has been reported to have an accelerating effect on Mg dissolution. It is also reported that the secondary phase of $Mg_{17}Al_{12}$ is the highest trigger phase [32].

Song et al. They conducted a study that pit corrosion is particularly related to secondary phases. It is known that Mg alloys with high Al content have higher corrosion resistance and less alloys containing rare earth elements. In the study, deep pits were formed, where the secondary phases dissolved first, then the Mg matrix near the secondary phases dissolved, and finally the starting point of the dissolved secondary phases [33].

Intergranular corrosion; It is a type of corrosion that occurs at grain boundaries due to secondary phases. Secondary phases or segregation are more likely to occur at grain boundaries. Here grain boundaries usually disappear [34].

Filiform corrosion; usually occurs on the metal surface. Paint etc. Galvanic cells active on protective metal surfaces cause filiform corrosion. In the initial stage, after the hole-shaped corrosion, it spreads as a filiform depending on the oxygen density on the surface [35].

Cleft corrosion; It is rare in Mg alloys. Hydrolysis reaction triggers this type of corrosion that starts in cracks in a narrow area. Mg hydroxide increases the effect between crack and Mg [36].

Stress corrosion; It is the case for extruded and extruded Mg alloys, and can also be seen in fast-cooled cast alloys. It is formed in humid air, high water, $NaCl + K_2CrO_4$ solution, $NaBr$, Na_2SO_4, $NaCl$ solutions. There are two types of theory as mechanisms, the first includes the preferential attack model, the film break model and the tunnel theory, and the other includes the crack process and the hydrogen breakage theory. Morphologically, it is classified as Intergranular and grained grains [36].

2.9.1. Effects of Alloy Elements on Corrosion Behavior of Mg

Al; Among the AZ alloys of the AZ series, especially the AZ31 alloy has the lowest corrosion resistance. It also contains optimum properties in terms of both mechanical and corrosion resistance. Formation of $Mg_{17}Al_{12}$ phase increases in AZ series with

increasing amount of Al. It is known that the increasing $Mg_{17}Al_{12}$ secondary phase increases metal loss and also stress corrosion cracks appear more [37].

Mn; Up to 5% (wt.) For pure Mg, Mn has little effect on corrosion resistance. In Mg-Al-Zn alloys, Al8Mn5, Al6Mn and Al4Mn type secondary phases contribute to corrosion resistance. Here, impregnated elements such as Fe are taken from the structure [37]

Zn; It is known that MgxZny type secondary phases weaken the corrosion resistance of Mg due to local cathodic behavior [37].

nd; Mg_3Nd is formed in binary Mg-Nd alloys and shows a more effective cathodic behavior compared to pure Mg. As a result, it acts as a local cathodic region and leaves an ever-increasing cathodic effect with increasing Nd amount. Despite this, it makes less increase in metal loss compared to La and Ce. Another difference is that it has higher atomic percentage compared to $Mg_{12}Ce$ and $Mg_{12}La$. The Nd element improves the corrosion resistance of the AZ series Mg alloys by creating secondary phases of type Al-Nd and Al-Mn-Nd. Another contribution is the formation of a surface film, but little work has been done on this subject [37].

Gd; The effect of Mg alloys on corrosion resistance is still lacking. Al_2Gd and Al-Mn-Gd secondary phases are formed in Mg-Al alloys. Here, while consuming Al, the volume fraction of the secondary phase $Mg_{17}Al_{12}$ decreases. It can be said that this situation has some effect on reducing cathodic reactions. However, the mixed microstructure and decreasing Al content of Gd-added Mg alloys still leave question marks in corrosion behavior. Long-term tests may be helpful to clarify the situation [37].

Liu et al. Y, Gd and Nd examined the effect of twinning on the corrosion properties of Mg alloy, which contains rare earth elements. It is stated that micro-galvanic corrosion occurs between the twin and the matrix, which causes both faster dissolution in Mg and the formation of surface film. The interaction of twin and surface films under

prolonged immersion test conditions has been said to cause an increase in the corrosion resistance of the alloy [38].

Wan et al. have studied how ultra-fine grains affect the corrosion resistance of the M-Gd-Y-Zr alloy. Extremely fine grains have been reported to ensure that MgO films remain more durable on the surface, thereby contributing to corrosion resistance. Increased grain boundaries here reduce stress and the oxide clings to the tighter surface [39].

Ca; Yang et al. They investigated the effect of Ca element on Mg-Al-Mn alloy corrosion resistance. It has been reported that there is thinning of the grains with increasing amount of% Ca, but in the first case it increases after decreasing corrosion resistance. It is said that with the addition of 2% Ca (Mg, Al) the 2Ca phase is discontinuously dispersed at the grain boundaries and the strongest resistance against corrosion is gained in this alloy. Here, these secondary phases pretend to be self-sacrificing and delay Mg corrosion [40].

Y; Baek et al. They investigated the effect of Y addition on Mg-Al-Ca alloy corrosion resistance. It has been reported that corrosion resistance develops with the addition of Y, where secondary phases containing Al are eliminated and replaced by new phases such as Al_2Y [41].

La; For the Mg-Al alloys, La improves the corrosion behavior as Al-La containing leafy secondary phases make the $Mg_{17}Al_{12}$ secondary phase more spherical and continuously dispersed. In addition, this creates a thinned microstructure and more anti-corrosion film layer [37].

PART 3

EXPERIMENTAL STUDIES

3.1. MATERIALS

3.1.1. Casting

In this recent study, AZ31 Mg alloy and modified AZ31 Mg alloys were studied as the main material. The raw materials used for production are given in Table 3.2. Pure Mg, Al pure, pure Zn alloys from Turkey gauges are supplied from China. For the production, a special low-pressure gravity die casting method was used (Figure 3.1) and the casting conditions given in Table 3.1 were complied with. Pure Mg was first introduced into the stainless-steel crucible. After reaching a temperature of 775 ° C, after a waiting period of 1-hour, pure Al and gauge alloys were added to the ladle. Meanwhile, the molten metal in the crucible was continuously stirred. The final alloy addition was added to the pure Zn crucible and after 10 min stirring the molten metal was injected into stainless steel metal molds having a temperature of 355 ° C under 2-4 atm.
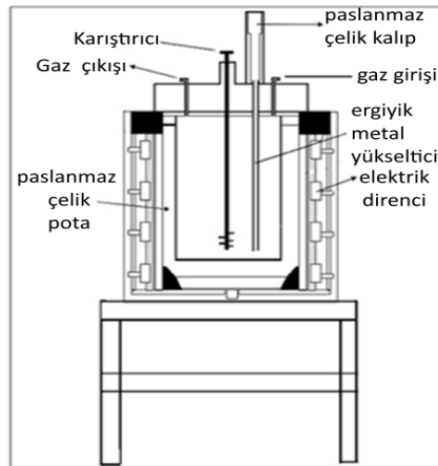
Figure 3.1. Diagram of low-pressure gravity die casting furnace.

Table 3.1.Casting conditions.

Protective gas	Melting temperature (° C)- Standby time (min)	Mold temperature (° C)	Runner temperature (° C)	Casting gas pressure (Atm)
Argon	775-60	350	350	2-3

Table 3.2.Raw materials used for production (% by weight).

Raw material	Mg	Al	Zn	Mn	Ca	Ce
Purified Mg	%99,99	----	-----	----	----	---
Purified Al	----	%99,98	-	---	---	---
Purified Zn	----	----	%99,989	---	---	---
Mastar Mn	%90	---	---	%10	-	-
Mastar Ca	%70	-	-	-	%30	-
Mastar Ce	%70	-	-	-	-	%30

The chemical contents of the produced alloys are given in Table 3.3. Rigaku ZSX Primus II device belonging to XRF laboratory of Karabük University Iron and Steel Institute was used for chemical analysis.

Table 3.3. The chemical contents of the produced alloys.

Alloy groups	Materials	Al%wt	Zn%wt	Mn%wt	Ca %wt	Ce %wt	Mg%wt
AZ31	AZ31.	2,94	0,987	0,131	-	-	Bal.
Ca	1Ca.	2,85	1,02	0,14	0,98	-	Bal.
Ce	0,2Ce	2,91	0,97	0,10	-	0,20	Bal.
	0,5Ce	2,93	1,03	0,12	-	0,39	Bal.
	1Ce	2,93	1,02	0,20	-	0,88	Bal.

3.1.2. Rolling

After casting, billets with dimensions of 120x36x12 mm were applied for homogenization heat treatment at 395-410 °C for 23-24 hours. In order to prevent metal oxidation during homogenization and homogeneous temperature distribution, the materials were embedded in sand. Homogenized materials were hot rolled with parameters in Table 4.4. Here, 15% (total 11 passes) section constriction was applied in each pass. Inter-pass materials were stored in a furnace at 395-410 °C for 5-6 minutes. After the narrowing total 83% of the section, billets with initial thickness of 12 mm was reduced to 2 mm thickness.

Table 3.4. Rolling parameters.

Rolling Temp. (°C)	Thickness Reduction per pass (%)	Rolling speed (m/min)	Total pass number	Total thickness reduction (%)	Initial and final thickness (mm)
400	15	1,5	11	83,3	12-2
		4,7			
		10			

3.2. CORROSION TEST

Immersion tests were implemented with 3.5% Sodium chloride mix at 25°C. The output of corrosion test were removed using 180 g l-1 CrO_3 for 1 minute in ultrasonic cleansing machine and drained by ethonal before mass loss measure. Morphology of the alloys was examined by SEM after immersion test.

3.3. WEAR TEST

The behaviour of dry sliding wear of the SP applied and MAO coated specimens was determined proving a AISI 52100 steel ball of 6 mm diameter. Test procedure was set up according to ASTM G-133. The wear tests were executed at medium conditions at

three different loads of 1N, 2N and 5N with an vacillate magnitude of 8 mm and at a sliding velocity of 5 mm s^{-1} for a sliding distance of 50m. Surface roughness and wear depth measurements were performed with a Mitutoyo profilometer. The worn surfaces of samples after wear test were examined by SEM. Further, characterization of the wear trails and the wear wreckage was accomplished in SEM with energy disperse spectra (EDS) analysis tool.

3.4. SURFACE ROUGHNESS TEST

The surface roughness, Ra, of the rolling direction on samples was computed handling surface profilometer (Mitutoya- SVC3200S4 model machine) according to ISO 1997 and the surveyed boundary was about 0.08 mm and three reiterations were attended for a moderate value.

3.5. HARDNESS TEST

Hardness tests were carried out in the BMS brand brinell hardness tester based on the brinell hardness method, using a 2.5 mm diameter ball under 187.5 kg load in accordance with the TS-EN-ISO 6506-1 standard in KBU Iron and Steel Institute Micro and Macro Hardness measurement laboratory. At least 3 measurements were taken from each material.

3.6. SAMPLE PREPARATION

Casting form of the produced alloys, homogenized and acetic-picral (70ml ethanol, 5ml acetic acid, 5g picric acid and 10ml pure water) ether were prepared for post-mill microstructure examinations. Before the etching process, sanding process with sanding papers of 600, 800, 1000, 1200, 2500 and polishing with 1μm diamond suspension and 1μm felt were performed.

3.7. MICROSTRUCTURE

3.7.1. Optical Microscope Images

Casting of the produced alloys, homogenized and post-mill microstructure investigations were done with Nikon Eclipse MA200 model optical microscope in Karabük University (KBU) Iron and Steel Institute Metallography laboratory

3.7.2. Scanning Electron Microscope Images

Casting of the produced alloys, homogenized and post-mill microstructure investigations were done with Carl Zeiss Ultra Plus Gemini Fesem model scanning electron microscope device in SEM laboratory. In addition, energy distribution spectrometer (EDS) studies were carried out on the same SEM device.

3.7.3. Grain Size and Twinning Fraction Analysis

Grain size analysis was calculated according to ASTM E112 standard from 200X magnification optical microscope pictures. SEM pictures with 500X magnification were used to calculate the twinning fraction and spot calculations were performed according to the ASTM E562-02 standard.

3.8. CHEMICAL AND TEXTURE ANALYSIS

3.8.1. X-ray Fluorescence (XRF) Analysis

Rigaku branded ZSX Primus II model XRF devices in the KBU Iron and Steel Institute XRD-XRF laboratory, were used to determine the chemical contents of casted samples.

3.8.2. X-ray Diffraction (XRD) Analysis

Ultima IV model XRD devices in the KBU Iron and Steel Institute XRD-XRF laboratory were used to determine the phases-texture of the produced alloys. XRD graphics were taken in the copper targeted XRD device in the range of 15-90 °. Missing pole figure measurements were obtained from the peaks (0002), (10-10), (10-11) and (10-12) and maximum texture strength and distributions were revealed using the MTEX toolbox.

PART 4

RESULTS

This section contains the results of test and analysis presented as Table and Figures in following parts.

4.1. MICROSTRUCTURE

4.1.1. LOM images

In Figure 4.1. It shows optical pictures of AZ31 - Ca and AZ31 - Ca-Ce Group Mg alloys. Here, Ce changed the structure of the AZ31 - Ca Mg alloy, which generally contains homogeneous equiaxed grains, into heterogeneous and different sized beads. As it can be seen in Figure 4.1, while the fine and coarse grains are heterogeneous, the grains are larger with the addition of 0.5% Ce, although with the addition of 1% Ce, equiaxed grains still exist according to the AZ31-Ca Mg alloy. Optical images of AZ31 Mg alloy with 0.2% Ce addition show equiaxed grains and twinning formed in some coarse grains. However, recrystallized grains could not be detected from the optical microscope pictures of 1Ca-1Ce. However, it has been observed that the materials that have been deformed at the rolling speeds of 4.7 m / min and 10 m / min contain equiaxed grains and twinning formed in the grains and equiaxed grains and new recrystallized grains formed around these grains. The optical image images of materials that have undergone deformation of 15% per pass at 4.7 m / min and 10 m / min of AZ31 Mg alloys with addition of 1% Ce show the grains where dense twinning occurs and many homogeneously distributed recrystallized grains. However, the optical image of the material that has undergone 15% deformation at a rolling speed of 10 m / min shows heterogeneously dispersed recrystallized grains and equiaxed grains without twinning.
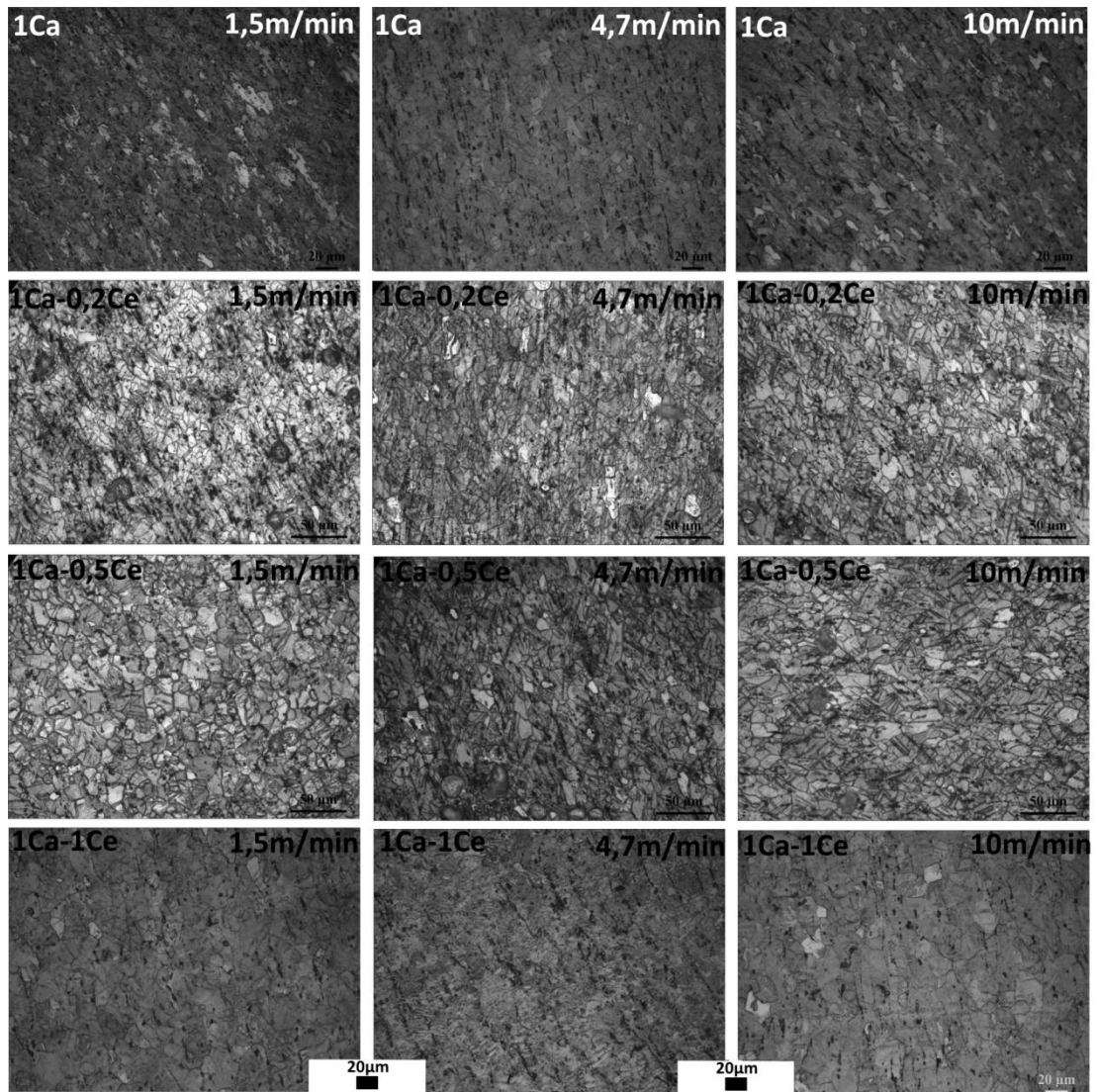
Figure 4.1. LOM images of rolled samples.

4.1.2. SEM Images
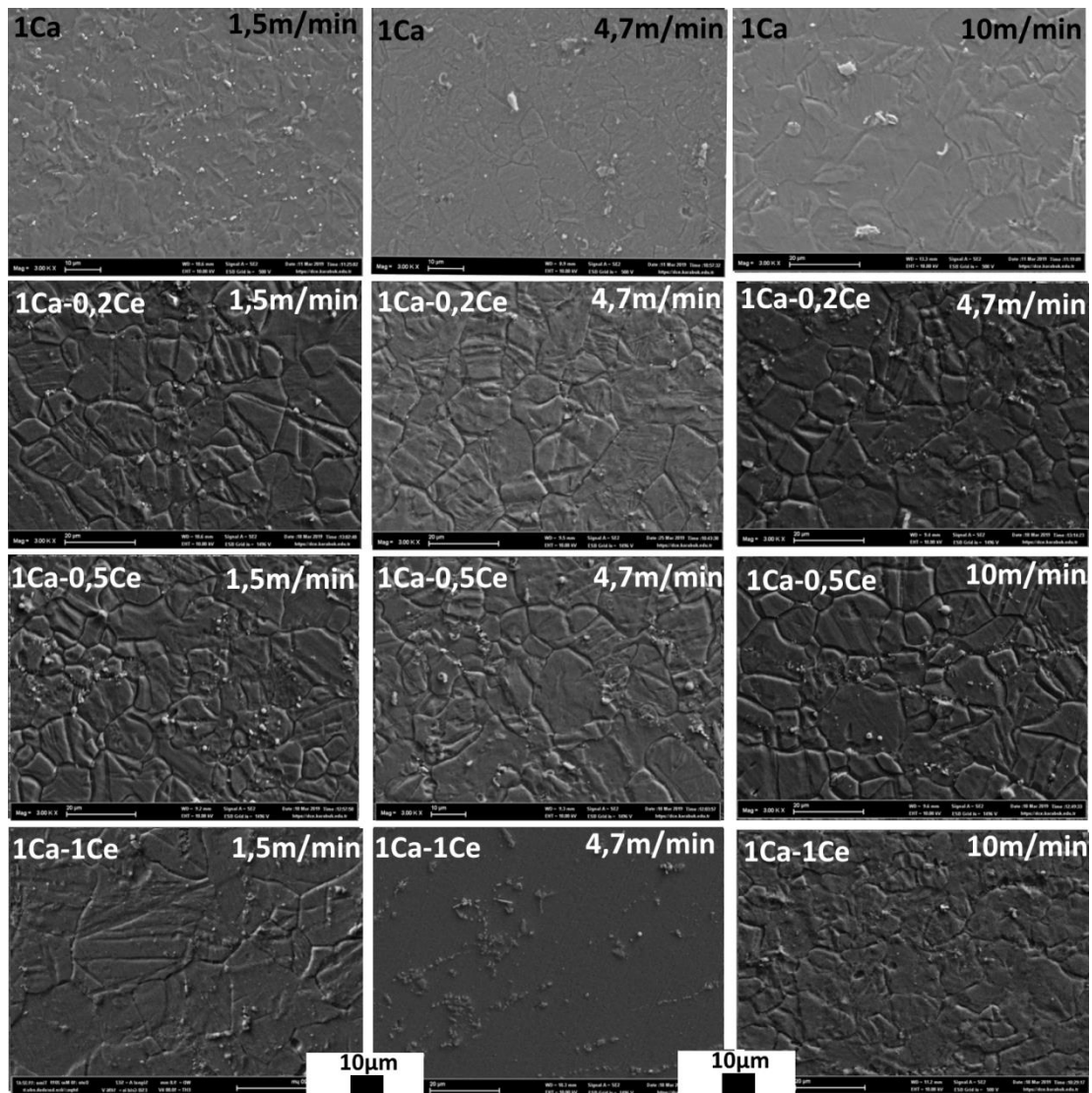
Figure 4.2. SEM images of rolled samples.

As can be seen in Figure 4.2., polygonal and spherical shaped secondary phases are formed in a wide range of dispersed AZ31-1Ca Mg alloys that have undergone 15% deformation per pass at 1.5 m / min, 47 m / min and 10 m / min rolling speed. Besides, there are larger spherical shaped secondary phases compared to the 4.7 m / min rolling speed at 10 m / min rolling speed. Despite this, AZ31-1Ca Mg alloys, which have undergone 15% deformation at 4.7 m / min and 10 m / min rolling speed, contain thin spherical shaped secondary phases formed in a certain area, dispersed and dispersed at wide intervals. As it can be seen in Figure 4.2, it is lined in the form of a large mixed

shape, thin string at the grain boundaries, dispersed with a wide range, respectively, in 1Ca - 0,2Ce Mg alloys, which are subjected to 15% deformation per pass at 1.5 m / min, 47 m / min and 10 m / min rolling speed, and finely polygonal shaped homogeneously dispersed secondary phases were formed. Despite this, 1Ca - 0,2Ce Mg alloys that have undergone 15% deformation at the rolling speed of 1.5 m / min, 4.7 m / min and 10 m / min contain thin spherical shaped secondary phases formed in a certain area and dispersed at wide intervals. It is seen that secondary solutions are aligned along the grain boundaries and dissolved in the matrix with increasing rolling speed. As can be seen in Figure 4.2., 1.5 m / min, 47 m / min and 10 m / min rolling speed, 15% deformation per pass, 1Ca - 0,5Ce Mg alloys are arranged in the form of thin beads at the grain boundaries and distributed in a wide range, finely spherical homogeneously dispersed secondary phases were formed. Despite this, 1Ca - 0,2Ce Mg alloys, which have undergone 15% deformation at 4.7 m / min and 10 m / min rolling speed, contain homogeneous grain boundaries accumulated in very fine grain boundaries and fine spherical secondary phases dispersed in the matrix at narrow intervals. As can be seen in Figure 4.2, at 1.5 m / min, 47 m / min and 10 m / min rolling speed, 15% deformation per pass, 1Ca - 1Ce Mg alloys, narrow spherical shape, thin spherical shape and thin polygonal, homogeneously dispersed in matrix, respectively. shaped homogeneously dispersed secondary phases are formed. Despite this, 1Ca - 1Ce Mg alloys that have undergone 15% deformation at the rolling speed of 1.5 m / min, 4.7 m / min and 10 m / min, have a spherical shape formed in the grain boundaries, a homogeneously distributed thin spherical shape and homogeneously distributed in wide intervals. contains spherical shaped secondary phases. Here, it is seen that secondary solutions are arranged along the grain boundaries and distributed in the matrix with increasing rolling speed.

4.1.3. Average Grain Size and Twins Fraction

Table 4.1. Avarage grain size and twins fraction of rolled samples.

Average Grain size (AVS)			
Materials	Rolling Speed		
	1.5 m/Min	4.7 m/Min	10 m/Min
1 Ca	15,1	13,9	7,8
1Ca-0.2 Ce	14,8	17,7	15,2
1Ca-0.5 Ce	15,4	19,1	16,8
1Ca-1 Ce	26,3	20,1	16,3
Twins Fraction			
Materials	Rolling Speed		
	1.5 m/Min	4.7 m/Min	10 m/Min
1 Ca	0,200	0,186	0,243
1Ca-0.2 Ce	0,243	0,300	0,271
1Ca-0.5 Ce	0,243	0,286	0,271
1Ca-1 Ce	0,186	0,186	0,229

4.2. HARDNESS MEASUREMENT

Hardness test results of AZ31-1Ca and AZ31-1Ca-Ce groups alloys with 15% deformation per pass and rolled at 1.5 m / min, 4.7 m / min and 10 m / min rolling speed are given at Table 4.2.

Table 4.2. Hardness values of rolled samples.

Hardness (HV)			
Materials	Rolling Speed		
	1.5 m/Min	4.7 m/Min	10 m/Min
1 Ca	65,4	64,3	66
1Ca-0.2 Ce	70,7	60	69,4
1Ca-0.5 Ce	68,4	63,1	71
1Ca-1 Ce	59,8	60,4	60,1

According to table results the increasing rolling speed of AZ31-1Ca Mg alloy with 15% deformation per pass, hardness vickers decreased firstly at 4,7 m/min however slightly rising was observed at 10m/min rolling speed. Similarly, the HV hardness of the Ca-Ce group alloys depending on the rolling speed showed diminishing at 4,7

m/min but, rising at 10m/min except 1Ca-1Ce alloy. The 1Ca-0.2Ce and 1Ca-0.5Ce alloys showed the lowest HV hardness value at 4.7 m / min rolling speed and the highest HV hardness value at 1,5 m / min and 10 m / min respectively. On the other hand, the highest HV hardness value of the 1Ca-1Ce alloy was measured at a rolling speed of 4.7 m / min.

4.3. CORROSION TEST RESULTS

The corrosion test results are given in Table 4.4. The corrosion rate and specific corrosion rate were calculated using of following formula.

Metal loss in unit area.

$$(g/cm^2) = metal\ loss/corroded\ area$$

Specific corrosion rate.

$$(g/cm^2.day) = metal\ loss\ in\ unit\ area/total\ corrosion\ time$$

4.4. WEAR TEST

The wear test results are given in Table 4.3. The wear rate and specific wear rate were calculated by using of following formula.

Wear rate; $V(mm^3) = \frac{2}{3}a.b.c$

Where a and b are the height and width of wear track and c is long of wear track.

Specific wear rate; $V(mm^3/m) = wear\ rate\ /\ d.N$

Where d is the total distance of wear, and N load in newton

Table 4.3. Wear rate of rolled samples.

Wear rate (g/m)			
Materials	Rolling Speed		
	1.5 m/Min	4.7 m/Min	10 m/Min
1 Ca	0,006918301	0,0035	0,005898693
1Ca-0.2 Ce	0,000372475	0,000178609	8,23338E-05
1Ca-0.5 Ce	0,000350773	7,93087E-05	0,000387731
1Ca-1 Ce	0,002382353	0,001588235	0,002856209

Table 4.4. Corrosion rate of rolled samples.

Time (hrs)	1Ca, 15% R			1Ca-0.2Ce, 15% R			1Ca-0.5Ce, 15% R			1Ca-1Ce, 15% R		
	1.5 m/min	4.7 m/min	10 m/min	1.5 m/min	4.7 m/min	10 m/min	1.5 m/min	4.7 m/min	10 m/min	1.5 m/min	4.7 m/min	10 m/min
0	0,0000	0,0000	0,0000	0,0000	0,0000	0,0000	0,0000	0,0000	0,0000	0,0000	0,0000	0,0000
3	0,0039	0,0027	0,0022	0,0015	0,0010	0,0016	0,0021	0,0017	0,0008	0,0037	0,0043	0,0021
9	0,0147	0,0220	0,0108	0,0043	0,0049	0,0054	0,0048	0,0045	0,0040	0,0200	0,0301	0,0168
12	0,0276	0,0710	0,0235	0,0094	0,0115	0,0100	0,0087	0,0097	0,0088	0,0665	0,0769	0,0608
24	0,0419	0,1080	0,0391	0,0196	0,0263	0,0185	0,0185	0,0178	0,0234	0,1696	0,1576	0,1346
48	0,0738	0,1470	0,0639	0,0485	0,0549	0,0398	0,0536	0,0295	0,0554	0,2816	0,2490	0,2079
72	0,0964	0,2007	0,0762	0,0696	0,0743	0,0593	0,0556	0,0690	0,0631	0,4108	0,3414	0,3723
Area (mm^2)	164	295	473	316	331	388	482	448	303	420	346	312
Area (m^2)	1,638E-04	2,954E-04	4,729E-04	3,162E-04	3,314E-04	3,876E-04	4,817E-04	4,484E-04	3,032E-04	4,198E-04	3,456E-04	3,118E-04
g/hrs	2,27E+00	4,10E+00	6,57E+00	4,39E+00	4,60E+00	5,38E+00	6,69E+00	6,23E+00	4,21E+00	5,83E+00	4,80E+00	4,33E+00
g m^{-2} day^{-1}	1,96E+02	2,26E+02	5,37E+01	7,34E+01	7,47E+01	5,10E+01	3,85E+01	5,13E+01	6,94E+01	3,26E+02	3,29E+02	3,98E+02

PART 5

DISCUSSION AND CONCLUSIONS

Because of their low density and high specific strength, magnesium alloys have received great interest as structural materials for applications in the automotive and aerospace industries [29]. However, low corrosion resistance is still main deficiency of Mg alloys which could be solved by alloying, coating or heat treatment processes [42] and [31]. To get finer grains, rolling especially is utilized to form the billet from high thickness to thin sheets. The twins are that the main deformation mechanism of rolling deteriorates the corrosion resistance of wrought Mg alloys because of the fact that stresses resulted from twins boundaries impart site to cathodic corrosion [31] and [43]. Moreover, the secondary phases of Mg17Al12 are the second cathodic corrosion contributor for Mg alloys which is formed finer and distributed non-homogenous inside the matrix and on grains boundaries [42]. In addition, the alloying with Ca is suggested to improve the oxidation resistance of Mg alloys due to it has more affinity to oxidation than Mg that acts as a barrier during the corrosion of Mg [40]. Further, rare earth elements (REMs) is another option to change of secondary phases, where the Ce has higher electronegative than Mg to compound with Al which resulting in more stable phase to corrosion and non-homogeneously distribution of Mg17Al12 could be replaced Ce-Al include secondary phases mostly showing regular shapes on grain boundaries [44]. In this study, to improve the commercially widespread Mg alloy of AZ31 the Ca and Ce elements were added to composition following hot rolling was utilized to get finer grains and homogeneous secondary phases on microstructure. The corrosion resistance of produced materials was tested at %3,5 NaCl solution at room temperature. Further, to understand the Ce amount on corrosion resistance of AZ31 was investigated systemically where LOM, SEM and XRD characterization methods were used.

5.1. IMMERSION CORROSION TEST RESULTS

The immersion test results of the investigated alloys are exhibited in Figure 5.1. At the first test period the inclinations of corrosion rate belonging to alloys are similar for 9 hours. Rising of metal loss after 9 hours was observed, and the higher amount was detected on 1Ca alloy deformed at 1.5m/min rolling speed. The increased inclination of corrosion rate endured up to 12 hours. Afterwards the inclination did not show any higher rising. Most alloys illustrated a similar trend between 12 and 48 hours. However, the inclination line of corrosion rate decreased until the end of the test for all samples. During the immersion tests, the highest corrosion resistance was obtained with 1Ca-0.5Ce alloy deformed at 1,5 m/min. As mentioned above, Ce mostly diffuses into the matrix where the solutes of Ce have a significant influence on the corrosion behavior of the material due to the galvanic effect occurring softly between the matrix and the grain boundaries [5, 8]. On the other hand, the poorest resistance to corrosion was detected in 1Ca alloy deformed at 1,5 m/min which has fine and continuously distributed Al-Ca rich secondary phases highly accelerate corrosion. Ce compounds with Al, thus eliminates the stable $Mg_{17}Al_{12}$ secondary phases from the structure which are replaced by Al-RE3 types [9].
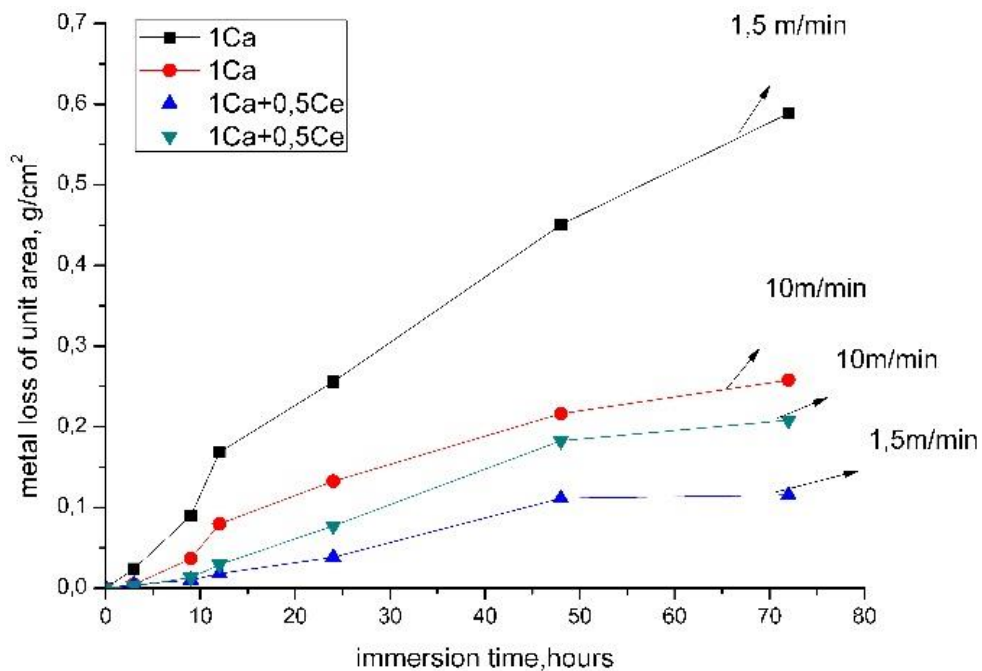

Figure 5.1. Immersion corrosion test results of the investigated alloys.

5.2. AVERAGE GRAIN SIZE AND TWINS TEST RESULTS

The average grain size results show that the finer grains of 7,8 µm were obtained for 1Ca alloy deformed at 10m/min rolling speed. As to compare the effect of the rolling speed on grain size, the higher rolling speed imparts finer grains to 1Ca added alloys, although the finer grains obtained by 1Ca-0,5Ce added alloys after 10m/min rolling speed. As for the twins, both alloys showed an increasing of twins fraction along with the rising of rolling speed. Moreover, the more highly twins density is introduced on 1Ca-0,5Ce added alloy deformed at 10m/min rolling speed (see Fig.5.2).
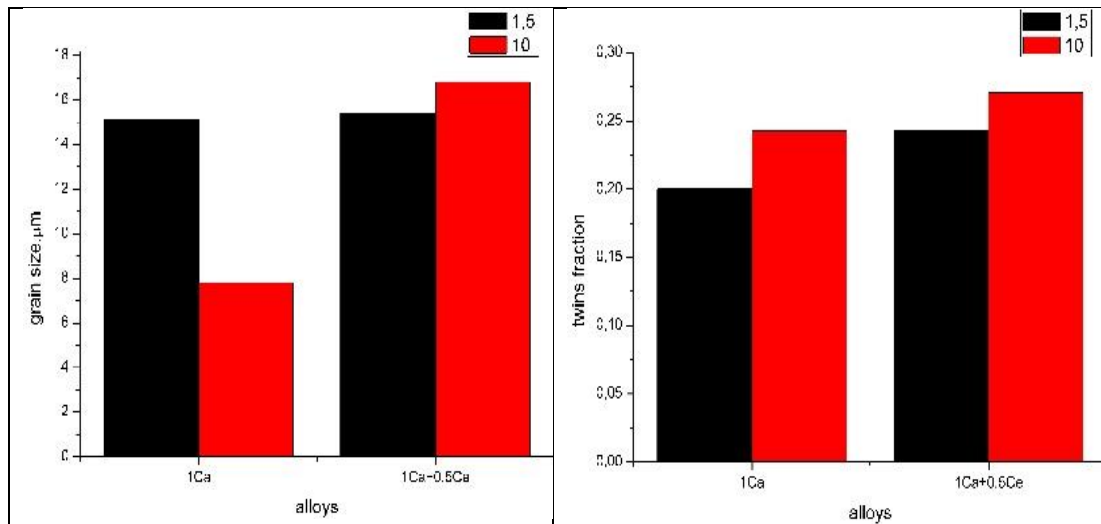

Figure 5.2. Avarage grain sizes and twins fractions of investigated alloys.

Magnesium alloys are one of the light materials due to their low density of 1,74 g/cm3 which give them an important advantage in using a structure material, especially in automotive and airspace vehicles parts [45] and [46]. Moreover, the properties of Mg alloys to be listed in order excellent damping capacity, good machinability, and high thermal conductivity. However, the wear resistance is a poor point of Mg alloys needing to be developed in dry or corrosive conditions [47] and [48]. To improve the wear resistance of mg alloys, alloying, coating, and heat treatment were utilized [49]. Rare earth elements can be used as an effective alloying method to enhance many properties of Mg alloys [50] and [42]. As to Ca that it brings about excellent mechanical properties, good corrosion resistance and superior thermal stability [8]. As for Ce that it leads to excellent corrosion resistance and good formability to Mg alloys

[37]. Although many studies to investigated of rare earth elements on wear behavior of Mg alloys is generally limited on as-cast or composite materials, the wrought Mg alloys added rare earth elements are still under discussion [49] and [45]. This study is aiming to examine the effect of Ca and Ce on wear behavior of hot-rolled AZ31 Mg alloys. Moreover, how the change of rolling speed affecting the wear resistance was investigated.

Fig.5.3 shows that the LOM images of investigated alloys. As seen in Fig.5.3., the grains of all samples mainly was formed as equiaxed after the rolling process. However, the average grain size of samples is different based on the rolling speeds. As we look at LOM images of AZ31-1Ca alloy, lower rolling speed gives rise to larger grains and besides more black points distributed mainly inside of grains when the rolling speed is 1,5 m/min (see Fig.5.3a). On the other hand, the twins that activated during rolling more occupied the microstructure at a higher rolling speed of AZ31-1Ca alloy (see Fig.5.3b). As regards the Ce addition to AZ31-1Ca alloy, the grains were formed as larger. Moreover, Ce added alloy that deformed at 10m/min shows larger grains and also contains more twins. The twins calculations of investigated samples illustrate that the higher rolling speeds activate the more twins formations for both alloy groups (see. Fig.5.3d and 5.3b).
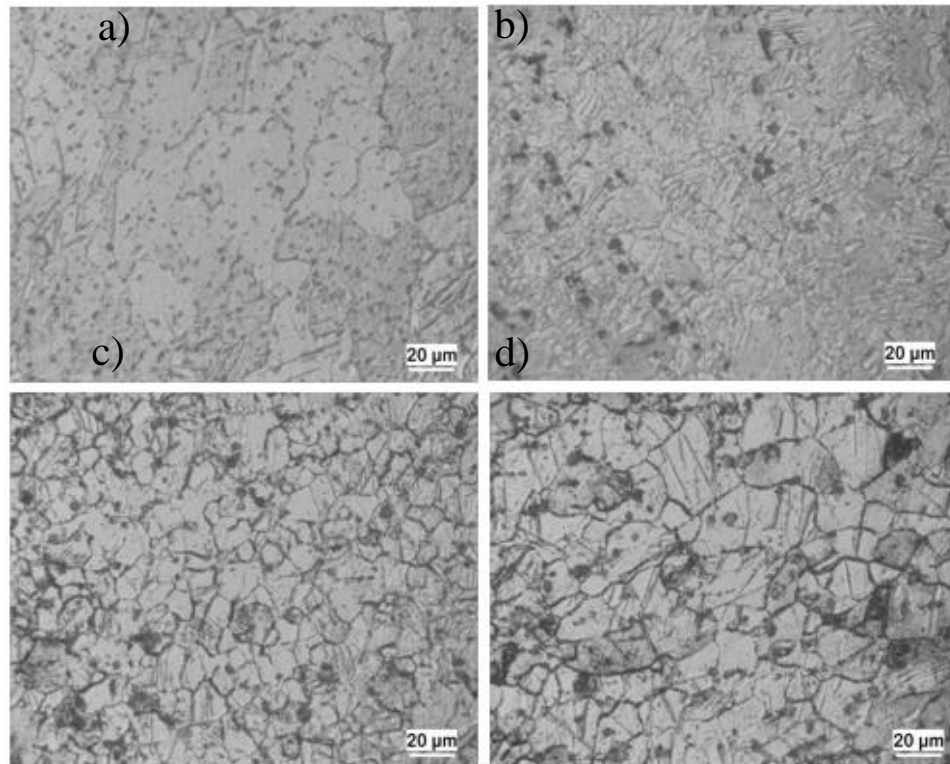
Figure 5.3. LOM images of AZ31-1Ca alloys deformed with a) 1,5m/min and b) 10m/min and AZ31-1Ca-0,5Ce alloys deformed with, c) 1,5m/min and d) 10m/min rolling speeds.

The SEM images of investigated alloys were present in Fig.5.6. The formation and distribution of secondary phases were examined by using these micrographs. As seen in Fig.5.6., the secondary phases of 1Ca that deformed at 1.5m/min rolling speed is finer and homogeneously distributed inside grains and grain boundaries both surface and cross-section. However, the size of secondary phases was enlarged when the rolling speed is 10m/min, where the distribution of larger secondary phases especially was placed on grains boundaries (see Fig.5.6.). Ce added materials contain more homogeneously distributed equiaxed grains, although the secondary phases of rolled at 1,5 m/min formed as larger size and placed on grain boundaries.

Mass percent (%) — a)

Spectrum	Mg	Al	Ca	Mn	Zn
1	31.85	45.39	20.64	0.07	2.05
2	24.31	35.15	32.48	2.56	5.51
3	42.45	34.83	19.17	1.30	2.24
4	38.61	29.82	26.07	0.95	4.54

Mass percent (%) — b)

Spectrum	Mg	Al	Ca	Mn	Zn
1	2.80	42.54	0.60	51.60	2.46
2	96.68	1.71	0.11	0.05	1.45
3	43.73	26.60	0.47	28.77	0.43
4	58.56	20.12	15.57	1.62	4.13

Mass percent (%) — c)

Spectrum	O	Mg	Al	Ca	Mn	Zn	Ce
1	19.77	16.67	35.77	24.33	0.52	2.86	0.08
2	19.87	71.73	4.24	1.57	0.00	2.58	0.00
3	6.13	88.94	1.83	0.07	0.00	2.24	0.79
4	12.00	25.03	34.95	25.51	0.50	2.03	0.00

Mass percent (%) — d)

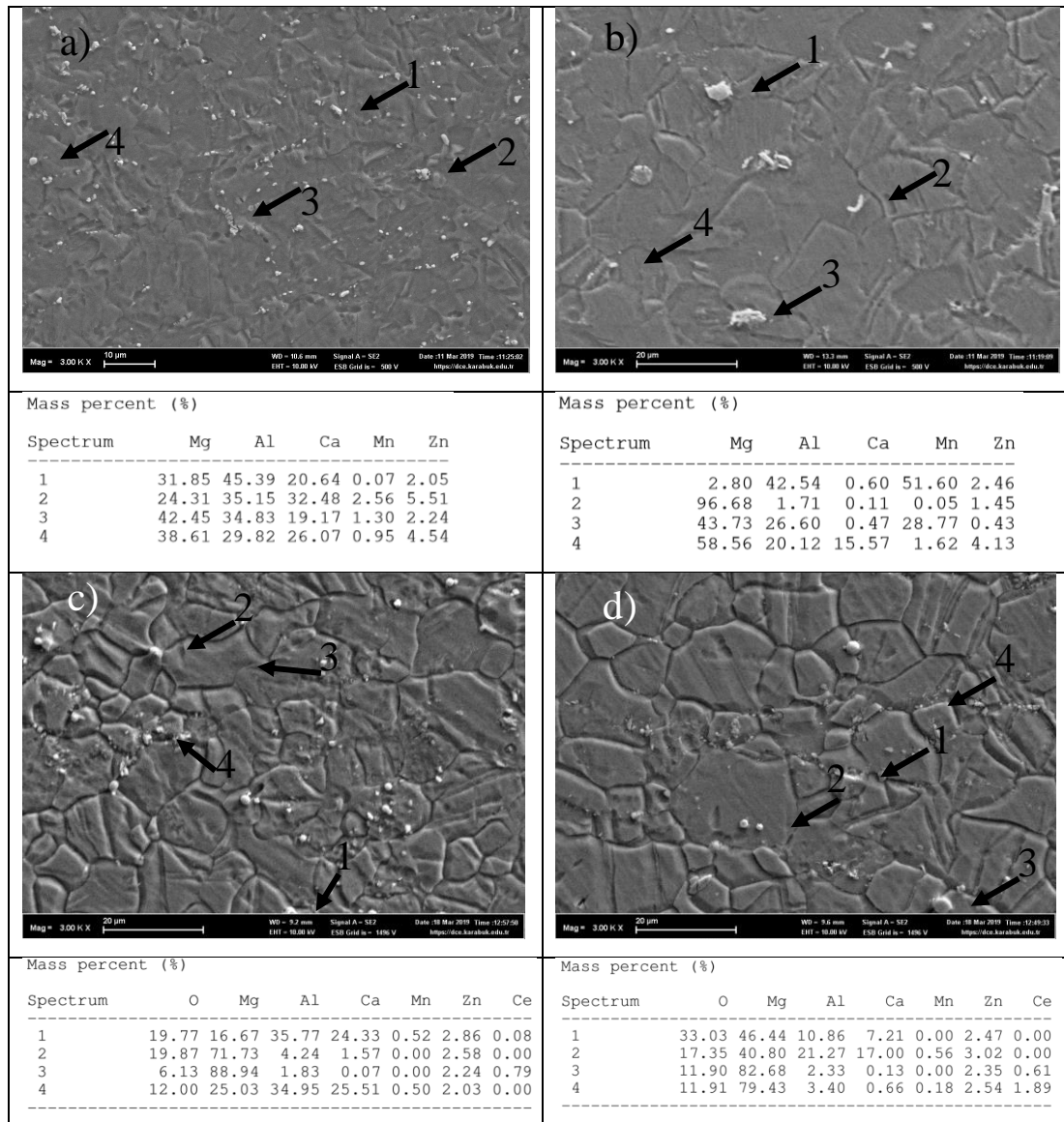| Spectrum	O	Mg	Al	Ca	Mn	Zn	Ce
1	33.03	46.44	10.86	7.21	0.00	2.47	0.00
2	17.35	40.80	21.27	17.00	0.56	3.02	0.00
3	11.90	82.68	2.33	0.13	0.00	2.35	0.61
4	11.91	79.43	3.40	0.66	0.18	2.54	1.89

Figure 5.4. SEM images and EDX results of AZ31-1Ca alloys deformed with a) 1,5m/min and b)10m/min and AZ31-1Ca-0,5Ce alloys deformed with c) 1,5m/min and d)10m/min rolling speeds.

The EDX examination shows that the secondary phases of Ca added alloy of deformed at 1,5m/min rolling speed was formed as a small spherical shape which dominantly Al-Ca rich. However, the rising of rolling speed to 10m/min solved generally smaller sized secondary phases in the matrix where Al-Mn rich secondary phases that were introduced mostly site on grain boundaries have a larger size and complex or rectangular shapes. However, a small number of the finer and spherical shaped secondary phases were detected on twins boundaries. When we examine Ce added AZ31-1Ca alloys, the Ce mostly has been solved in the matrix of 1Ca-0,5Ce alloy

deformed at 1,5m/min rolling speed due to the chemical composition of secondary phases does not include Ce element or trace amount. However, the same alloy contains spherical shaped secondary phases that contain Ce elements, where the rolling speed is 10m/min, more than rolled at 1,5 m/min speed.

5.3. HARDNESS TEST RESULTS

Fig.5.5. shows that the microhardness test results of investigated samples. As seen Fig.5.5, the hardness of AZ31-1Ca and AZ31-1Ca-0,5Ce alloys was changed positively by the increasing of rolling speed. Moreover, the highest hardness was obtained with 0,5 Ce added material which deformed at 10m/min rolling speed. The hardness could be increased with the formed smaller grains or more twins formation that gives rise to hindering of dislocation motion freely along slip direction [51]. However, twins boundaries impart to more blocking effect on the dislocation motion than grain boundaries.
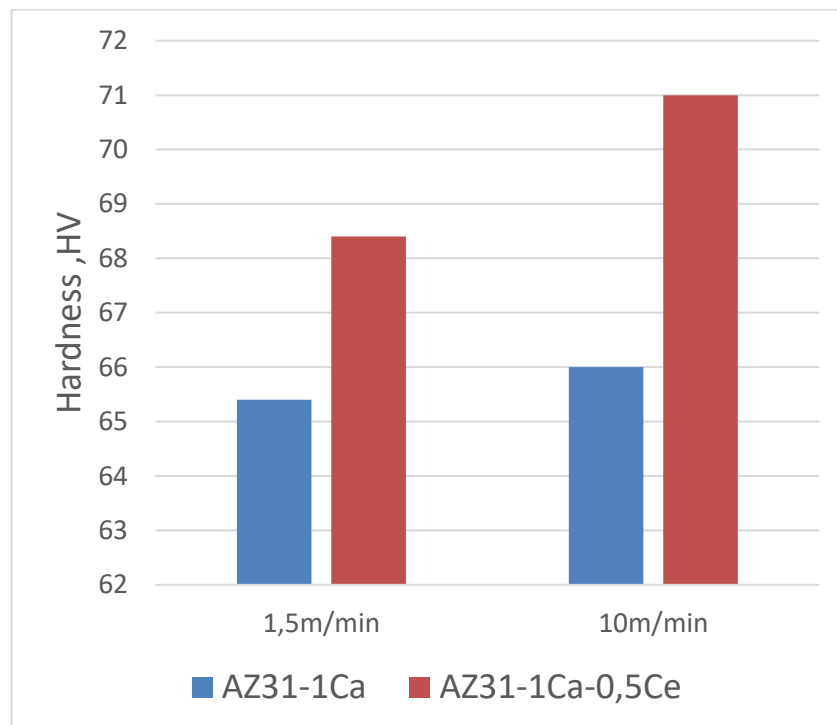

Figure 5.5. Hardness (HV) test results of investigated alloys.

5.4. WEAR TEST RESULTS

The wear test results of investigated alloys were given in Fig.5.8. As seen in Fig.5.8, metal loss of AZ31-1Ca alloy is higher when the material is deformed with lower rolling speed. As to AZ31-1Ca, the wear result is confirmed with the hardness results, where the higher hardness gives rise to lower metal loss during wear test. The wear resistance of AZ31-1Ca alloy was improved with the addition of Ce which is extremely lower when we compare it with AZ31-1Ca as seen Fig.5.6 however, the effect of rolling speed on the wear resistance of AZ31-1Ca-0,5Ce alloy is not proportional with the hardness results in which the 10m/min rolling speed have higher metal loss than 1,5m/min. The secondary phases distributed more homogeneous and bigger sized on the matrix of AZ31-1Ca-0,5Ce alloy deformed at 1,5 m/min than 10m/min rolling speed. The resist of secondary phases could be responsible for the wear behaviour of AZ31-1Ca-0,5Ce alloy with 1,5m/min rolling speed.
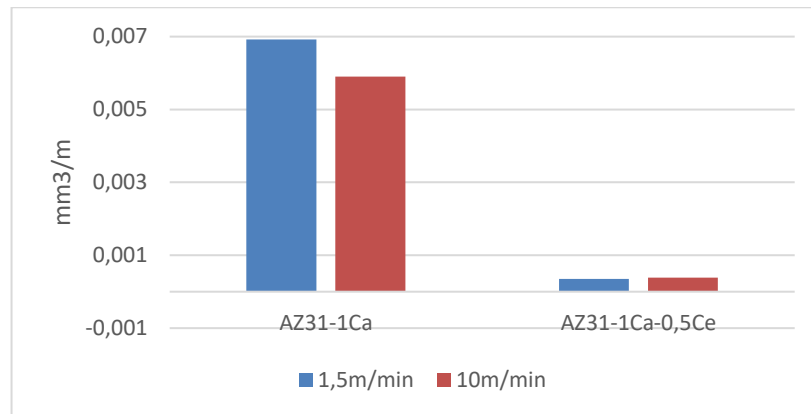

Figure 5.6. Metal loss (mm3/m) after wear test of investigated alloys during 120 m of 2N load.

When looking at the optical microscope pictures of rolled materials, 4.7 m / min rolling speed thin coaxial grains, however, 10 m / min rolling speed brought larger coaxial grains to the microstructure. During the rolling, the results of the grain sizes affected the rolling speed. As it is known, with the increased rolling speed, the material is exposed to more strain rate per pass. While the Mg alloys evaluate this strain rate energy as twinning in the first passes, they spend it in the form of recrystallization in the next passes and the size of these recrystallized grains. Here, the material had

coarser grains because of the size of the recrystallized grains at a rolling speed of 10 m / min. As a result of the SEM examination, it is seen that the secondary phases (white color) are larger and especially denser at the grain boundaries at a speed of 4.7 m / min. However, it is seen that the increasing rolling speed, in addition to the increasing deformation energy, thinned the secondary phases more and spread to both the matrix and grain boundaries. In addition, some secondary phases examined through EDS appear to be rich in Ca-Al. It was analyzed that the secondary phase at 4.7 m / min rolling speed contained larger and more Ca but finer and less Ca at 10 m / min rolling speed.
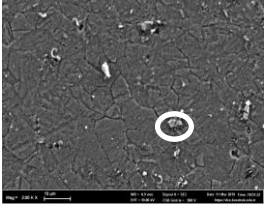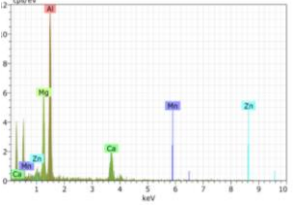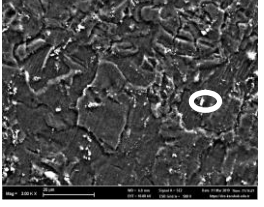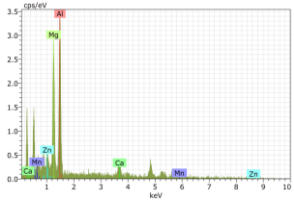
Rolling speed	OM	SEM	EDS	
4,7 m/min				(O) 23,4
				(Mg) 14,5
				(Al) 34,8
				(Ca) 24,4
10 m/min				(Zn) 7,12
				(Mg) 29,1
				(Al) 46,2
				(Ca) 16,4

Figure 5.7. LOM and SEM images of AZ31-1Ca invesitgated samples.

Figure 5.8. Wear and Hardness results of investigated samples.

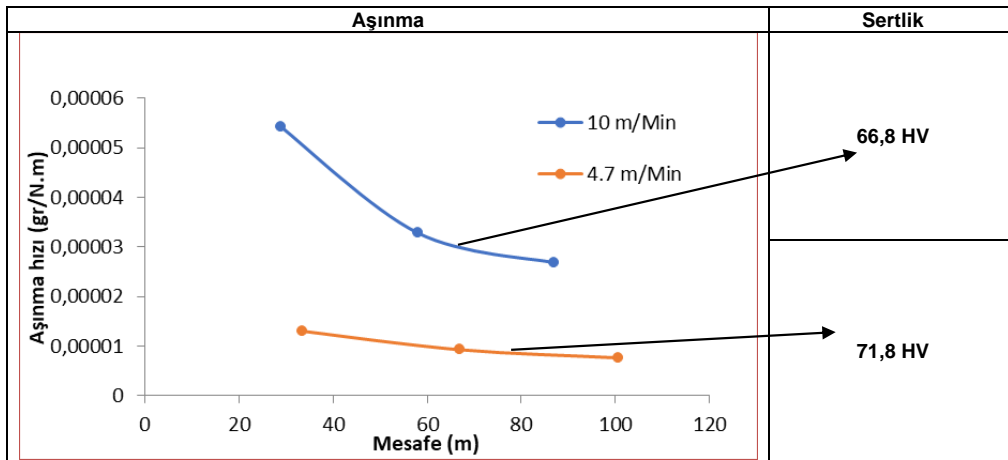As seen in the figure after the abrasion test, the rolled material at 10 m / min rolling speed was more worn than the rolled material at 4.7 m / min rolling speed. This result is supported by the hardness test support. Rolled material with a higher hardness value of 4.7 m / min rolling speed showed more resistance to abrasion. Nevertheless, the rolled material at a rolling speed of 10 m / min showed poor wear behavior due to its softer structure.

The LOM images of investigated alloys were showed at Fig. 5.9. In addition, the average grain size of alloys was illustrated at Fig.5.12. As seen Fig.5.9, grains are almost similar when the amount of Ce in the range of 0,2% to 0,5% although, the more Ce than %0,5 increased the size of grains (See Fig.5.11).
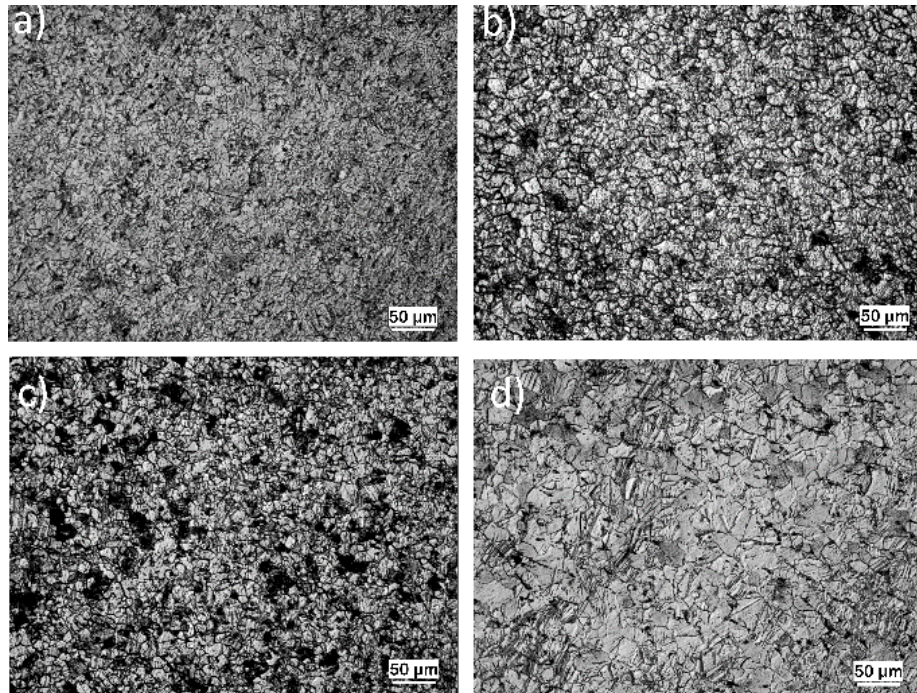
Figure 5.9. LOM images of sample a) AZ31-1Ca, b) AZ31-1Ca-0.2Ce, c) AZ31-1Ca-0.5Ce and d) AZ31-1Ca-1.0Ce.

The SEM images of investigated alloys were showed at Fig.5.12. The secondary phases distribution was similar for all samples as seen Fig.5.12. Same of them are inside of grains and the others on the grain boundaries. However, the size of the secondary phases was different. AZ31-1Ca alloy includes finer secondary phases which mostly distributed separately on the grain boundaries partially inside of grains.

However, when the 0.2%Ce is added to AZ31-1Ca alloy, the secondary phases clearly are becoming larger and majority of them located on grain boundaries. Moreover, as the amount of Ce is 0.5%, same secondary phases that formed finer and placed inside of grains. On the other hand, many of the secondary phases dissolved in matrix when the amount of Ce is 1.0%.

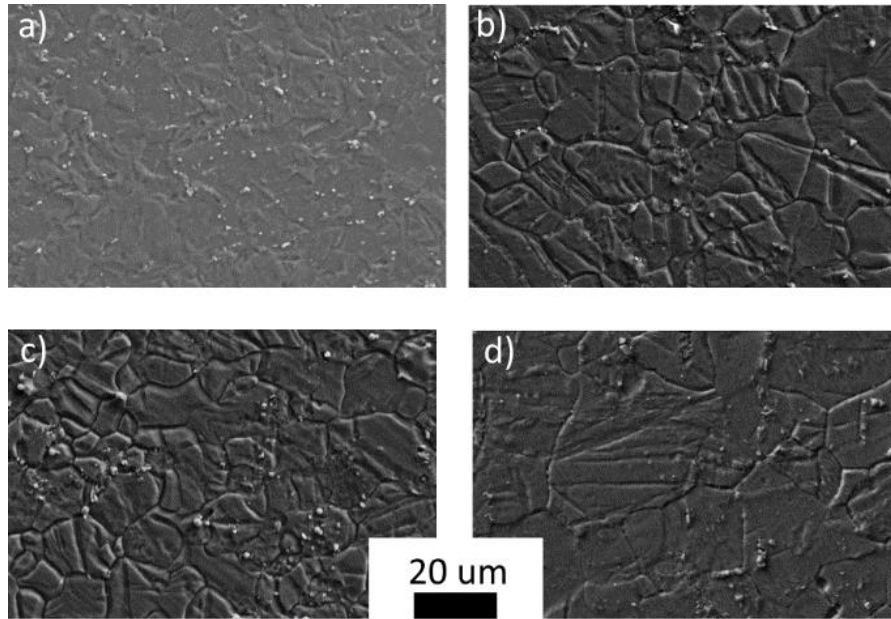Figure 5.10. SEM images of sample a) AZ31-1Ca, b) AZ31-1Ca-0.2Ce, c) AZ31-1Ca-0.5Ce and d) AZ31-1Ca-1.0Ce

5.5. TWINS FRACTION

As presented this Fig.5.11. twins more occurred when the amount of Ce is 0,2% (AZ31-1Ca-0,2Ce), however the more Ce addition limited the twins formation on microstructure. Further, twins fraction is obtained by addition of 1.0%Ce (AZ31-1Ca-1Ce) as a minimum amount (See Fig. 5.11).

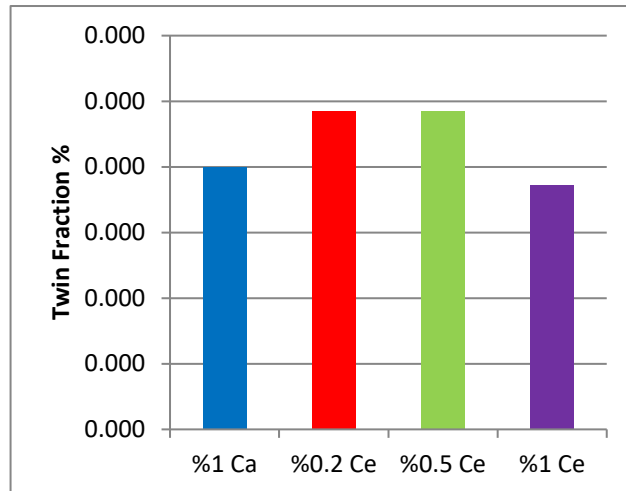Figure 5.11. Twins Fraction of samples.

5.6. AVERAGE GRAIN SIZE

Average grain size of samples was presented at Fig.5.12. As seen Fig.5.12, Ce addition does not make an important difference on size of grains when it is in the range of AZ31-1Ca-0.2Ce to AZ31-1Ca-0.5Ce. However, as Ce is AZ31-1Ca-1Ce, the average size of grains is the biggest [54].
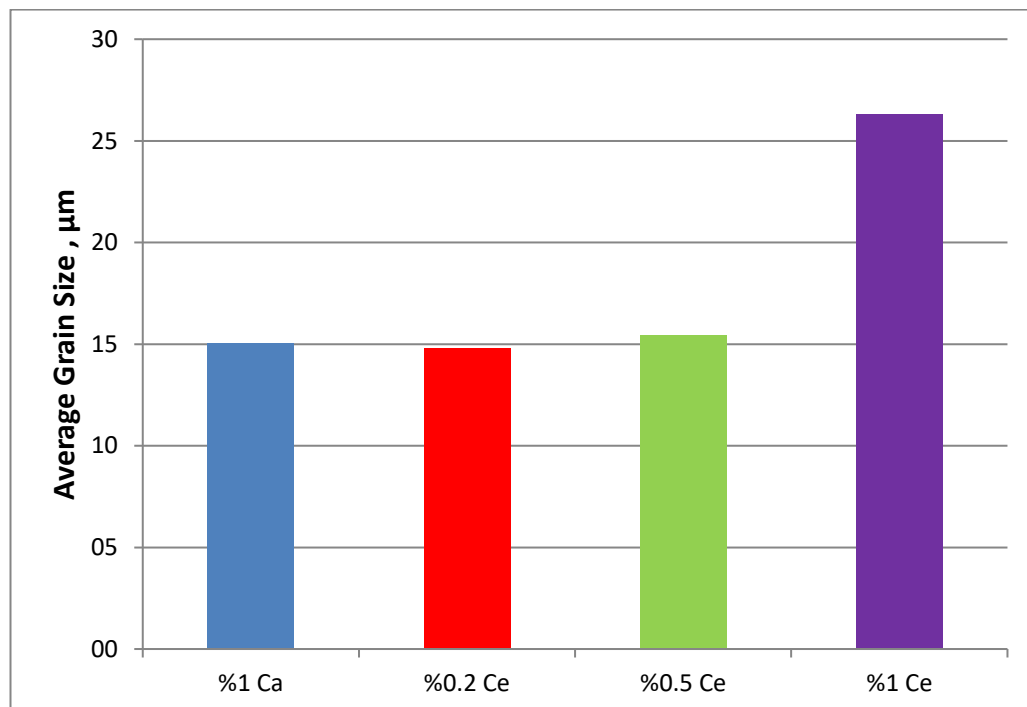

Figure 5.12. Average grain size of samples.

5.7. IMERSION CORROSION TEST

The immersion test results of studied materials were showed at Fig. 5.13. As seen in Fig.5.13., the metal loss of AZ31-1Ca-1Ce alloy occurred excessively. However, the lowest metal loss was observed at AZ31-1Ca-0,5Ce alloy.
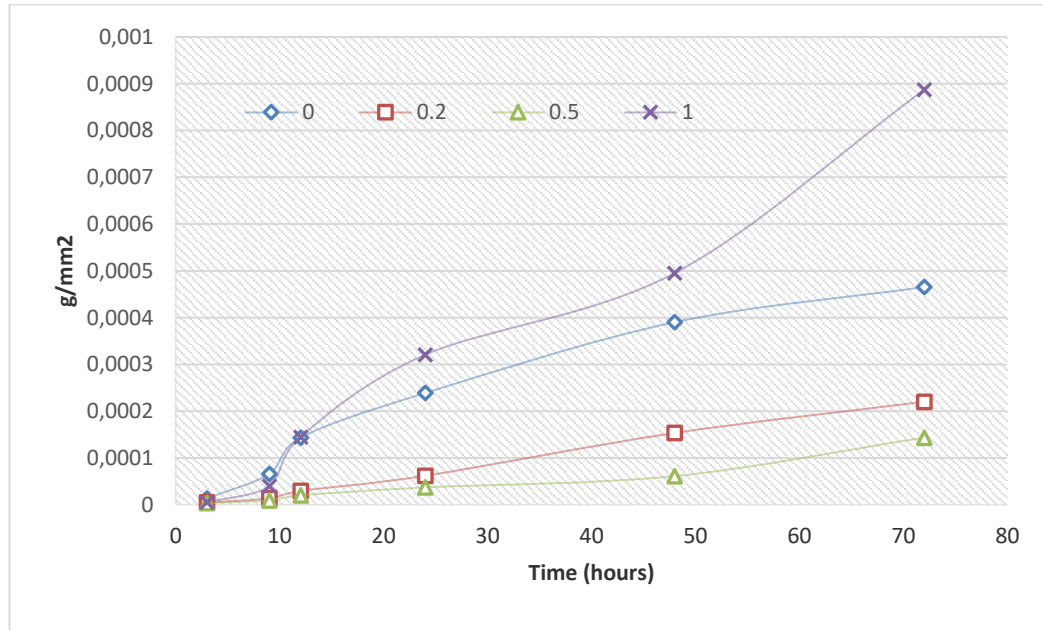
Figure 5.13. Effect of Immersion corrosion test results of samples on Ce Content.

5.8. SEM IMAGES FTER IMMERSION CORROSION TEST

Fig. 5.14. illustrates the SEM images of AZ31-1Ca-0.2Ce and AZ31-1Ca-0.5Ce added alloys after immersion test in 3.5% NaCl solution for 72 hours. As seen this Fig.5.14, corroded section of samples mostly occurred on matrix material. However, the secondary phases resist the corrosion and protect their stable condition. The main and important difference of secondary phases of AZ31-1Ca-0.2Ce and AZ31-1Ca-0.5Ce is the location and size of them. AZ31-1Ca-0.2Ce added alloy have bigger sized secondary phases and they are accumulated on grain boundaries. However, AZ31-1Ca-0.5Ce added alloy includes finer ones and they mostly distributed inside of grains [32].

Figure 5.14. SEM images a) 1Ca-0.2Ce and b) 1Ca-0.5Ce after immersion corrosion test.

5.9. Conclusıon

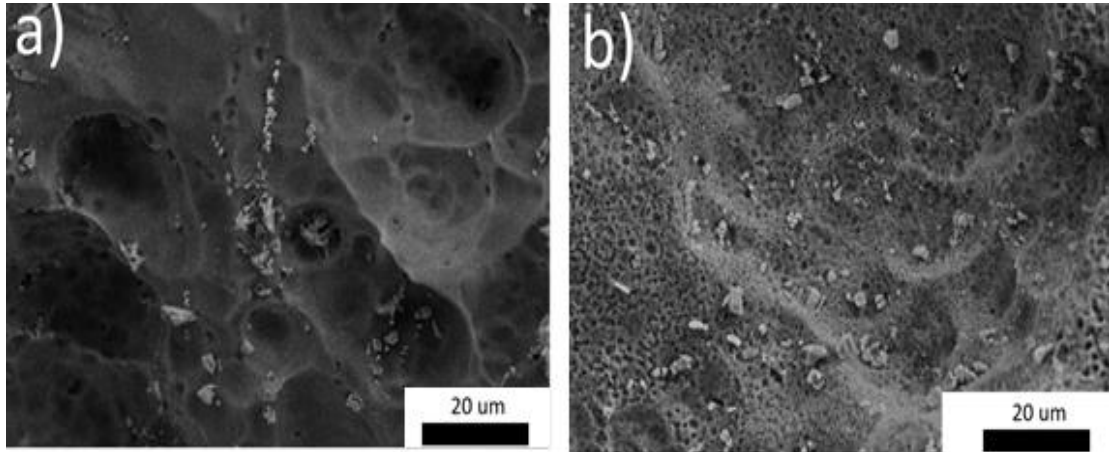- In this study, the Ce and rolling speed effected the corrosion resistance of AZ31-1Ca alloys was proved by microstructure analysis, where the solid solution of Ce element in a matrix made an important role as a dominant determiner to more stable it in %3,5 NaCl solution. Moreover, the rolling speed changed the size and shape of secondary phases distributed on grain boundaries when the rolling speed is 1,5m/min which controls the corrosion resistance positively.

- In this study, the Ce and rolling speed effected the wear resistance of AZ31-1Ca alloys was proved by microstructure analysis, where the solid solution of Ce element in a matrix made an important role as a dominant determiner to more stable it in wear test. Moreover, the rolling speed has changed the distribution and size of secondary phases which effected approximately minor scale to the wear resistance of investigated alloys which have the bigger size of secondary phases, the more it resists to wear.

- The grains of its alloy containing AZ31-1% Ca rolled at a rolling speed of 10 m/min are larger than that of the rolled at a speed of 4.7 m/min, and as a result it

54

has shown a lower value in hardness as well as more material loss as a result of the wear test.

- The average grain size is more dominant to determine of corrosion resistance than twins fraction. The distribution and size of secondary phases effect the corrosion resistance effectively where the larger and located on grain boundaries are desirable properties to obtain stronger corrosion resistance.

REFERENCES

1. Kainer, K.U. ”Magnesium Alloys and Technology”, *Wiley-VCH Verlag GmbH & Co. KG aA, Weinheim*, (2003).

2. Mordike, Friedrich, and Barry,” Magnesium Technology Metallurgy, Design Data, Applications”, *Springer*, (2006).

3. Luo, A., "Magnesium casting technology for structural applications", *Journal of Magnesium and Alloys* 1, 2-22 (2013).

4. Correa, and Becerra M., "Effect of Solute Elements on the Lattice Parameters of Magnesium", *Department of Mining, Metals, and Materials Engineering*, (2006).

5. Esmaily, M., Svensson, J.E., and Others, "Fundamentals and advances in magnesium alloy corrosion." *Cilt* 89. (2017).

6. Yang, Z., Li, J. P., Zhang, J. X., Lorimer, G. W., and Robson, J.,.”Review on research and developent of magnesium aaoys” *Acta Metallurgica Sinica*, (2008).

7. Cao, P., Qian, M. And Stjohn, D. H. "Grain coarsening of magnesium alloys by beryllium" *Scripta Materialia,* 647-651. (2004).

8. Rokhlin, L., and others, "Calcium-alloyed magnesium alloys" *Metal Science and Heat Treatment*: 164-169. (2009).

9. Luo, A. and Pekguleryuz, M.O., "Cast magnesium alloys for elevated temperature applications" *Journal of Materials Science,* 5259–5271. (1994).

10. *Jackson*, J.H., and others. "Magnesium-lithium base alloys - preparation, fabrication, and general characteristics" *Metals Transactions,*: 149-168 (1949).

11. Lunder, O., Aune, T.K. and Nisancioglu, K. "Effect of Mn additions on the corrosion behavior of mould-cast magnesium ASTM AZ91" *Corrosion,* 291-295. (1987).

12. Amirnejad, M., Rajabi, M. And Motavalli, A. "Effect of addition of Si on microstructure, mechanical properties,bio-corrosion and cytotoxicity of Mg−6Al−1Zn alloy" *Transactions of Nonferrous Metals Society of China,* 1755-1762 (2018).

13. Ben-Hamu, G., and others. "Microstructure and corrosion behavior of Mg–Zn–Ag alloys" *Materials Science and Engineering: A* 435-436: 579-587. (2006).

14. Hono, K., and others. "Towards the development of heat-treatable high-strength wrought Mg alloys". *Scripta Materialia,* 710-715. (2010).

15. Li, J., and others. "Effect of Zr modification on solidification behavior and mechanical properties of Mg–Y–RE (WE54) alloy" *Journal of Magnesium and Alloys,* 346-351. (2013).

16. Kirkland, N.T. and Birbilis. N. "Magnesium Biomaterials: Design, Testing, and Best Practice". Switzerland: *Springer*, (2014).

17. Xin Zhang, and others. "Phase equilibria on the ternary Mg–Mn–Ce system at the Mg-rich corner" *Journal of Alloys and Compounds,* 482:420–428. (2009).

18. Mezbahul-Islam, M., Mostafa, M. And Medraj, M. "Essential Magnesium Alloys Binary Phase Diagrams and Their Thermochemical Data" 2014 (2014).

19. Okamoto, H. "Ce-Mg (Cerium-Magnesium)". *Journal of Phase Equilibria and Diffusion*, 32.3 (2011).

20. Tekumalla, S. And others. "Mechanical Properties of Magnesium-Rare Earth Alloy Systems: A Review" *metals,* 1-39. (2014).

21. Wasiur-Rahman, S. And Medraj, M. "Critical Assessment and Thermodynamic Modeling of the Binary Mg–Zn, Ca–Zn and Ternary Mg–Ca–Zn Systems" *Intermetallics,* 17:847–864. (2009).

22. Shang, Lihong. "Effect of Micro Alloying on Microstructure and Hot Working Behavior for AZ31 Based Magnesium Alloy" *Montreal, Quebec, Canada : McGill University*, (2008).

23. Bahrami, A., and others. "Root Cause Analysis of Surface Cracks in Heavy Steel Plates during the Hot Rolling Process" *metals,* 9.7:801. (2019).

24. Yunpeng, Ding, and others. "Effect of rolling speed on microstructure and mechanical properties of as-cast AZ31B alloy under different reduction schedules" *Journal of Materials Processing Technology,* 161-173. (2016).

25. Fei, Gou, and others. "Influence of rolling speed on microstructure and mechanical properties of AZ31 Mg alloy rolled by large strain hot rolling" *Materials Science and Engineering,. A* : 383-389.(2014).

26. Di, Liu, Li Zuyan and Wang Erde. "Effect of rolling reduction on microstructure, texture, mechanical properties and mechanical anisotropy of AZ31 magnesium alloys" *Materials Science and Engineering, A*: 208-213. (2014).

27. Kim, W.J., and others. "Microstructure and mechanical properties of Mg–Al–Zn alloy sheets severely deformed by asymmetrical rolling" *Scripta Materialia,* 309-312. (2007).

28. Huang, Xinsheng, and others. "Texture and stretch formability of AZ61 and AM60 magnesium alloy sheets processed by high-temperature rolling" *Journal of Alloys and Compounds,* 94,102. (2015).

29. Wei, Y.H., and others. "Superplasticity and grain boundary sliding in rolled AZ91 magnesium alloy at high strain rates" *Materials Science and Engineering, A*: 107-115. (2003).

30. Imandoust, A., Barrett, C., Al-Samman, T., Inal, K., and El Kadiri, H.."«A review on the effect of rare-earth elements on texture evolution during processing of magnesium alloys" *Journal of Material Science,* cilt 52, no. 1, pp. 1-29, (2017).

31. Li, W. P., Zhou, H., Li, Z. F.. "Effect of gadolinium on microstructure and rolling capability of AZ31 alloy" *Journal of Alloys and Compounds,* 227–232. (2009).

32. Song, Guang-Ling. *Corrosion of magnesium alloys,* Cambridge: Woodhead Publishing Limited, (2011).

33. Feng, H., and others. "Effect of the second phases on corrosion behavior of the Mg-Al-Zn alloys" *Journal of Alloys and Compounds,* 2330-2338. (2017).

34. Song, Yingwei , Dayong Shan and En-Hou Han. "Pitting corrosion of a Rare Earth Mg alloy GW93" *Journal of Materials Science & Technology,* 954-960. (2017).

35. Man, Cheng , and others. "The Corrosion Behavior of Magnesium Alloy AZ31 in Hot and Dry Atmospheric Environment in Turpan, China" *International Journal of electrochemical science,* 8691-8705. (2015).

36. *Slabaugh*, W. H. And Morris Grotheer. "Mechanism of Filiform Corrosion" *Industrial and Engineering Chemistry,* 1014-1016. (1954).

37. Rong-chang, Zeng, and others."Review of studies on corrosion of magnesium alloys" *Transactions of Nonferrous Metals Society of China*, 763-771 (2006).

38. Gusieva, K., and others. "Corrosion of magnesium alloys: the role of alloying" *International Materials Reviews*, 169-194. (2015).

39. Liu, J., and others. "Effect of twins on the corrosion behavior of Mg–5Y–7Gd–1Nd–0.5Zr Mg alloy" *Journal of Alloys and Compounds*, 356-363. (2018).

40. Wan, Y., and others. "Enhanced strength and corrosion resistance of Mg-Gd-Y-Zr alloy with ultrafine grains" *Materials Letters*, 274-277. (2018).

41. Yang, J., and others. "Effect of Ca addition on the corrosion behavior of Mg–Al–Mn alloy" *Applied Surface Science,* 92-100. (2016).

42. Baek, S.M., and others. "Role of alloyed Y in improving the corrosion resistance of extruded Mg–Al–Ca-based alloy" *Corrosion Science*, 227-232. (2017)

43. Kara, İ. H., Ahlatcı, H., and Türen, Y., and Sun, Y., "Microstructure and corrosion properties of lanthanum-added AZ31 Mg alloys" *Arabian Journal of Geosciences,* cilt 11, p. 535, (2018).

44. Lee, J., Kim, S. Song, S. Lee, C., and Park, S., "Dynamic recrystallization behavior and microstructural evolution of Mg alloy AZ31 through high-speed rolling" *Journal of Materials Science & Technology,* cilt 34, pp. 1747-1755, (2018).

45. Liu, P., and others., "The effect of Y, Ce and Gd on texture, recrystallization and mechanical property of Mg–Zn alloys" *Journal of Magnesium and Alloys* 4.3:188-196. (2016).

46. Aydın, Fatih and Yavuz Sun., "Investigation of wear behaviour and microstructure of hot pressed TiB2 particulate reinforced magnesium matrix composites" *Canadian Metallurgical Quarterly*, 4 b:455-469. (2018).

47. Zhang, J.B., and others. "Influence of Ca-Ce/La synergistic alloying on the microstructure and mechanical properties of extruded Mg–Zn alloy" *Materials Science and Engineering: A* 708 : 11-20. (2017).

48. *Ilanaganar*, E. and S. Anbuselvan. "Wear mechanisms of AZ31B magnesium alloy during dry sliding condition" *Materials Today: Proceedings*, 628-635. (2018).

49. Asl, K., Masoudi, A. and Khomamizadeh, F.."The effect of different rare earth elements content on microstructure, mechanical and wear behavior of Mg–Al–Zn alloy" *Materials Science and Engineering, A* 527.7-8:2027-2035. (2010).

50. Cug, H. and Ahlatci, H.. "Effect of Zn and Mn Additions on the Wear Resistance Cast Alloy Mg-5%Al-1%Si" *Metal Science and Heat Treatment,* 59.7-8: 161-167. (2017).

51. Nouri, M., Sun X. and Li, D.Y. "Beneficial effects of yttrium on the performance of Mg–3%Al alloy during wear" *corrosion and corrosive wear,* 154-163. (2013).

52. Aydın, Fatih and Yavuz Sun. "Investigation of wear behaviour and microstructure of hot pressed TiB2 particulate reinforced magnesium matrix composites" *Canadian Metallurgical Quarterly*, 4 b.: 455-469. (2018).

53. Li, S., and others. "Grain Coarsening Behavior of Mg-Al Alloys with Mischmetal Addition". *Journal of rare earths*, 25.2:227-232. (2007).

54. Barnett, M.R. "Twinning and the ductility of magnesium alloys: Part I: "Tension" twins." *Materials Science and Engineering, A*: 1-7. (2007).

55. Guo, Li-li and Fujita, F. "*Effect* of deformation mode, dynamic recrystallization and twinning on rolling texture evolution of AZ31 magnesium alloys" *Transactions of Nonferrous Metals Society of China*, 1094-1102. (2018).

56. Zhanga, Xin, Dmytro Kevorkovb and Mihriban Pekguleryuza. "Stoichiometry study on the binary compounds in the Mg–Ce system—Part I" *Journal of Alloys and Compounds*, 361–367. (2009).

RESUME

Taher Ali Issa Yousef after he accomplished his elementary education. He completed high school education in Hay Al Andalos High School, after that, he started the undergraduate program at Tripoli University Department of Metallurgical and Materials engineering, faculty of nuclear and electronic engineering in 1982. In 2003, he started assignment as a Research Assistant at Belarussian National Technical University, at Department of Materials Technology in Mechanical Engineering, to complete M.Sc. degree. Later, He moved to Karabük University, where he has been still working as a Ph.D. student.

In addition to his academic career, he has gained substantial experience while working for Arabian Gulf Oil Company, Tripoli Research, and Development Center, and Al-jabel Algarbi University, Faculty of Engineering, Libya.